Stone Mountain Technologies, Inc.

Low-Cost Gas Heat Pump for Building Space Heating
DE-EE0006116

Final Report

November 25th, 2015

Revised October 11th, 2016

Prepared For:

Leon Fabick, Project Officer

U.S. DOE

Prepared By:

Michael Garrabrant

Christopher Keinath, PhD

Stone Mountain Technologies, Inc.

Johnson City, TN 37604

Team Members:

A.O. Smith Corporation

Milwaukee, WI

Gas Technology Institute

Chicago, Ill

ACKNOWLEDGMENTS & DISCLAIMER

The work presented in this report is the result of the hard work and dedication of dozens of individuals and small businesses. Roger Stout, David Firestine and Chuck Culver designed, assembled and tested solution pumps, breadboard heat pump systems, and the packaged prototypes. Janice Fitzgerald of A.O. Smith designed and tested the condensing gas heat exchanger. Paul Glanville, Yongfang Zhong, Daniel Suchorabski and Brian Sutherland of GTI completed combustion system development, evaporator modeling, packaged prototype testing and building energy modeling. SMTI also thanks the Department of Energy for funding and supporting this work regarding this breakthrough space heating technology.

This material is based upon work supported by the Department of Energy under Award Number DE-EE0006116.

EXECUTIVE SUMMARY

Gas-fired residential space heating in the U.S is predominantly supplied by furnaces and boilers. These technologies have been approaching their thermodynamic limit over the past 30 years and improvements for high efficiency units have approached a point of diminishing return. Electric heat pumps are growing in popularity but their heating performance at low ambient temperatures is poor. The development of a low-cost gas absorption heat pump would offer a significant improvement to current furnaces and boilers, and in heating dominated climate zones when compared to electric heat pumps. Gas absorption heat pumps (GAHP) exceed the traditional limit of thermal efficiency encountered by typical furnaces and boilers, and maintain high levels of performance at low ambient temperatures. The project team designed and demonstrated two low-cost packaged prototype GAHP space heating systems during the course of this investigation.

Led by Stone Mountain Technologies Inc. (SMTI), with support from A.O. Smith, and the Gas Technology Institute (GTI), the cross-functional team completed research and development tasks including cycle modeling, 8× scaling of a compact solution pump, combustion system development, breadboard evaluation, fabrication of two packaged prototype units, third party testing of the first prototype, and the evaluation of cost and energy savings compared to high and minimum efficiency gas options.

Over the course of the project and with the fabrication of two Alpha prototypes it was shown that this technology met or exceeded most of the stated project targets. At ambient temperatures of 47, 35, 17 and -13°F the prototypes achieved gas based coefficients of performance of 1.50, 1.44, 1.37, and 1.17, respectively. Both units operated with parasitic loads well below the 750 watt target with the second Alpha prototype operating 75-100 watts below the first Alpha prototype. Modulation of the units at 4:1 was achieved with the project goal of 2:1 modulation, which will allow for improved load matching. In addition, the energy savings analysis showed that a house in Albany, NY, Chicago, IL and Minneapolis, MN would save roughly 32, 28.5 and 36.5 MBtu annually when compared to a 100% efficient boiler, respectively.

The gas absorption heat pump achieves this performance by using high grade heat from the combustion of natural gas in combination with low grade heat extracted from the ambient to produce medium grade heat suitable for space and water heating. Expected product features include conventional outdoor installation practices, 4:1 modulation, and reasonable economic payback. These factors position the technology to gain significant market penetration, resulting in a large reduction of energy use and greenhouse gas emissions for residential space heating.

TABLE OF CONTENTS

1.0 INTRODUCTION

Natural gas is the primary means of heating homes in the U.S. Where available, natural gas is generally preferred due to its convenience (versus stoking solid fuel furnaces/boilers) and lower costs (versus fuel oil and bottled gas, e.g. propane). Site use of electricity, to drive resistance heating equipment and, more recently, electric heat pumps (EHPs), have steadily gained in popularity since the mid-1970s.

Space heating is the largest end use of natural gas in residences. With data from the most recent Residential Energy Consumption Survey [DOE EIA, 2009], total gas consumption for residential space heating is 29.5 billion therms, 63% of all residential natural gas consumption and 29% of all residential site energy consumption[1], resulting in 156 million metric tons of CO_2 emissions annually. Space heating represents between 50 and 67% of residential natural gas consumption depending on region, with higher proportions in the colder Northeast and Midwest. The distribution of heating fuel is highly regionalized, with effects of climate, utility pricing, and characteristics of housing stock all contributing. The majority of gas is consumed in the Cold and Very-Cold climate regions, with more than 5,400 heating degree days (HDD) and more than 9,000 HDD, respectively, with 57% of the natural gas used for space heating. An additional 28% of natural gas used for space heating is consumed in the Mixed-Humid climate region, with approximately 5,400 HDD. Thus, the majority of residential natural gas consumption in the U.S., at 54%, serves the space heating needs of homes in the Cold/Very-Cold and Mixed-Humid climate regions.

As residential space heating in the U.S. consumes a large amount of energy (primarily natural gas), it is a target for energy efficiency and carbon emission reductions. Minimum efficiency requirements and EnergyStar® qualifications have been slow to change. In 2015 DOE issued a revised final rule for a nationwide 92% AFUE minimum efficiency requirement [DOE, 2015] citing that half of products sold in Northern states were condensing efficiency and near half of certified products had an AFUE of 92% or greater. DOE is most recently considering a size-based standard, wherein “small” furnaces will not be subjected to a condensing-level minimum efficiency standard.

While the jump from non-condensing to condensing may be justified economically, even without the government/utility incentives which rapidly drove adoption from 1995 to 2008, incremental improvements in condensing efficiency from 90% to 98% AFUE are more difficult to justify. In their most recent final rulemaking, DOE estimates that the infrastructure costs of retrofitting a non-condensing with a condensing furnace can exceed $1,500, which depending on system efficiency yields payback periods of no less than 7 years [DOE, 2015].

The condensing efficiency furnace and boiler markets are mature, representing a large and increasing fraction of their respective markets. Conversely, the highest efficiency condensing equipment with an AFUE of 95% or greater often are not economically justifiable, as indicated by EnergyStar market penetration and exacerbated by low natural gas prices. Thus, pending regulatory pressures and broader economic realities converge at the lower range of condensing efficiencies, 90%-95% AFUE, leaving end users limited options for high-efficiency gas heating.

1 Natural gas consumed for space heating is the largest single end use of site energy for any fuel, more than all residential site electricity consumption for space heating, A/C, water heating, and refrigeration combined.

Electric heat pumps: The trend of gas heating in the majority of US homes appears to continue with the current state of low natural gas prices, as 60% of the 620,000 new single-family (SF) homes built in 2014 were heated by natural gas. The majority of new homes have installed warm-air furnaces since 1980. However, many new homes are heated with EHPs in milder climates where A/C is common. The advantages of EHPs are many-fold: potential for reduced heating costs, integrating cooling and heating systems with reversible heat pumps, and, where applicable, improving performance as a geothermal heat pump. Improvements in EHP technology, reduced EHP equipment costs, and lower new-construction heating loads (better insulation and building in milder climates) all drive this greater adoption of EHPs. EHP shipment data indicate that in addition to being an increasingly more preferred heating technology for new construction, that 2015 will likely be the year that more EHPs are shipped than warm-air furnaces [AHRI, 2015]. This indicates that EHP technology is increasingly preferred as a retrofit for existing homes in mild climates, retrofitting from gas heating or electric resistance heating.

EHPs, primarily as air-source heat pumps (ASHP), are growing in popularity due to improved efficiency, with introduction to EnergyStar in 1995 with a Heating Seasonal Performance Factor (HSPF) of 8.2 for split and 8.0 for packaged systems. Using a recently developed methodology outlined by Kim (2013), these correspond to a COP at 47°F of 3.86 and 3.81, respectively, which when computed on a source-energy basis yield COPs of 1.22 and 1.21 respectively[2]. As compared to standard electric heating equipment, these ASHPs offer significant savings and, especially in the case of ductless mini-split electric ASHPs, do not require significant retrofit investments.

EHPs are popular in milder climates and where local electricity rates are competitive (namely the South and the Pacific Northwest). As EHP technology improves, this is beginning to be the case in cold climates too, where gas heating is well established. As noted, homeowners in cold climates with gas heating and, perhaps just as importantly, utilities and governments seeking to promote equipment with improving energy efficiency are challenged by the following set of conditions:

- The "low-hanging fruit" is nearly picked, as condensing-efficiency furnaces and boilers are already well established in the climate regions 5, 6, and 7, and have been for almost two decades.
- Whereas 90-92% AFUE equipment can be cost-effective, incrementally higher condensing-efficiency furnaces and boilers are often not (Leslie, 2015)
- In the coming years, 92% AFUE may be required federally, severely limiting the opportunity to promote condensing-efficiency equipment with performance-based incentives (e.g. with EnergyStar differentiation).

In total, this market and regulatory pressure create an opening for gas heating equipment with an AFUE greater than 100%, namely a gas heat pump. This is most compelling in the cold climate regions, where savings potential is greatest and where saturation of condensing-efficiency products is greatest.

---

2 Primary/site energy conversion factor for US estimated as 3.16 (electricity) and 1.09 (natural gas), based on 2010 data from U.S. EPA Emissions & Generation Resource Integrated Database (eGRID).

Analogous to the Heat Pump Water Heater specification issued by the Northwest Energy Efficiency Alliance (NEEA), the Northeast Energy Efficiency Partnership (NEEP) has developed a more stringent requirement for cold-climate electric ASHPs wherein an HSPF of 9.0 or greater is required for multi-zone systems and 10.0 or greater for single-zone systems. These correspond to a site-basis COP at 47°F of 4.02 and 4.17 respectively, and on a source-basis 1.27 and 1.32 respectively [NEEP, 2014]. As part of ensuring sufficient performance at cold ambient temperatures, this specification includes the requirement that the ASHP operate with a site-basis COP of 1.75 or greater with a 5°F ambient temperature. *This drop-off in COP as a function of ambient temperature highlights a challenge of the vapor compression cycle, in which the heat pump COP and capacity are strong functions of ambient temperature.* Efficiency and capacity are reduced with colder ambient temperatures as, with a greater temperature lift required (T_{indoor} - $T_{outdoor}$, directly related to the refrigerant's $T_{condenser}$ - $T_{evaporator}$), the compressor must work harder delivering a higher pressure ratio. Often the reduction in capacity is partially or wholly augmented by resistance heating, part of this reduction in system COP.

Gas Absorption Heat pumps: The air-source gas-fired absorption heat pump (GAHP), uses an energy input (natural gas) to "pump heat" from the outdoors to an indoor conditioned environment. At the core of the GAHP is a group of heat exchangers, vessels, and a pump that comprise the "thermal compressor". The GAHPs that are currently commercially available are primarily models from the Italian manufacturer Robur, whose products and that of their few competitors are typically a) too large for residential applications and b) have equipment costs[3] greater than $13,500 [Delta Energy & Environment, 2014].

While currently available GAHP systems are prohibitive on a size and first-cost basis, their energy and cost saving potential is quite large. Assuming a baseline 78% AFUE furnace with 3% of input as parasitic electricity loads, the energy and operating cost savings for an EnergyStar rated electric ASHP (HSPF = 8.2) and a GAHP with an assumed seasonal AFUE of 140% with 6% of input as parasitic electricity loads are shown in Figures 1and 2 for several regions in the U.S. Annual residential heating loads are assumed for single-family housing [Huang, 1999], with locations ordered from largest to smallest left-to-right, nationwide source energy conversion factors are used, and local electricity-to-gas (E/G) price ratios are based on 2013 state-wide averages. Significant source energy and therm savings are achieved by the GAHP in comparison to the electric ASHP, even in mild climates. Due to the current period of depressed natural gas prices, significant comparative operating cost savings are also achieved, even in the Pacific Northwest with an E/G of 2.27. Using the local gas rates, these therm savings would yield between $2,550 (Texas) to $10,730 (Massachusetts) in savings over a 15 year period assuming a 4% average annual utility rate increase. As a result, even the extreme savings case in Boston would have difficulty justifying the aforementioned equipment costs when the baseline furnace installation is $2,200 [Leslie, 2015]. Therefore, to realize these large energy savings for this major natural gas end use, *a low-cost GAHP for cold climates is essential*.

The project team consists of ***Stone Mountain Technologies, Inc.,*** and major sub-contractors ***A.O. Smith Corporation*** (OEM partner) and the ***Gas Technology Institute (GTI)***. Project tasks include heat pump thermodynamic cycle optimization, heat exchanger and combustion system design, solution pump development/testing, fabrication and testing of a breadboard system, fabrication

3 Cost estimate excludes fees/markup associated with shipment to North America from EU and are scaled to GAHP size by 40%.

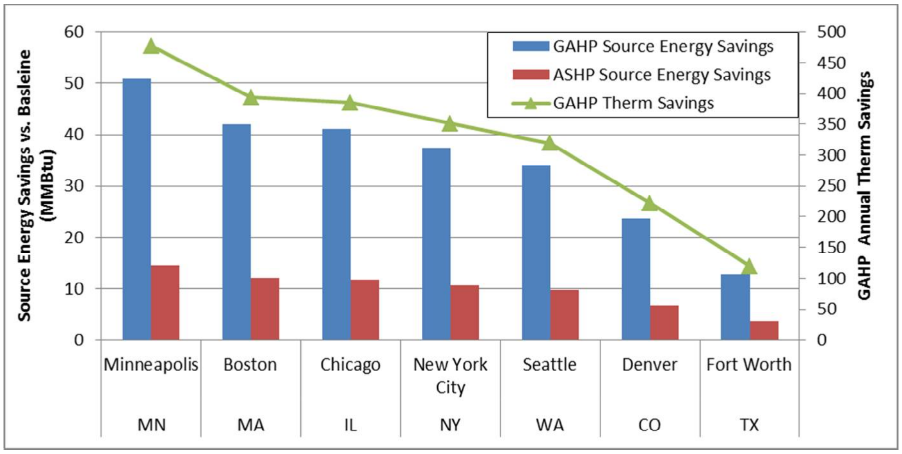

Figure 1: Source Energy and Therm Savings for GAHP vs. Electric ASHP and Baseline Gas Heating (GTI)

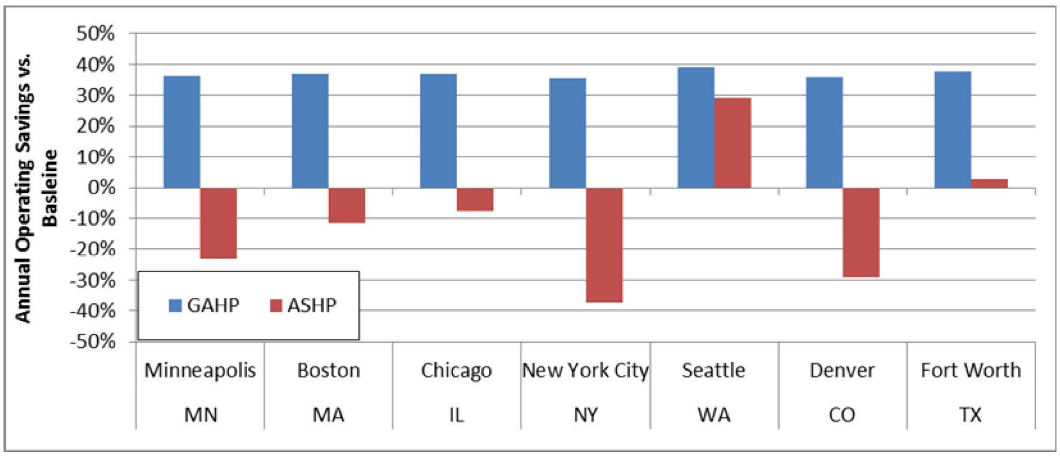

Figure 2: Estimated Operating Cost Savings for GAHP vs. Electric ASHP (GTI)

and testing of two packaged prototypes, and a cost and energy use comparison with commercially available technologies.

Through selection of the single-effect cycle and focus on easily manufactured components, the team seeks to demonstrate an economical GAHP, at a projected equipment price of 30-50% that of gas heat pumps currently available.

The packaged air-to-water GAHP, designed for outdoor installation, is sized at a nominal 80,000 Btu/hr output at 47°F ambient condition. Like other hydronic heating equipment (e.g. hot water boilers), the GAHP directly integrates with a hydronic heating system, such as in-floor radiant heating, but requires a hydronic air coil to integrate with a forced-air heat distribution system. It is sized for large residential applications, large single-family homes, retrofits into moderately tight envelopes, and as part of a combination space/water heating system. Additionally, in this size range it can serve small commercial heating loads, including commercial water heating.

2.0 SCOPE OF WORK AND PROJECT TASKS

Scope of Work: Thermodynamic cycle modeling was performed to investigate and optimize system performance. The resulting state points were used as inputs to component design models that provided physical dimensions for fabrication of the prototype heat exchangers and sizing information for the combustion system and solution pump. The prototype heat exchangers were installed on a breadboard facility, and tested to evaluate cycle and component performance. Testing was performed in an iterative approach. The solution pump was scaled up more than 8× its previous capacity. Building on the improvements made during the breadboard testing, two stand-alone packaged prototype units were developed, fabricated and tested. The first prototype was sent to GTI for third party testing in an environmental chamber and the second unit remained at SMTI for controls, performance and application optimization. Performance data was then used to compare the energy and utility cost savings of the gas absorption heat pump to representative high and minimum efficiency gas options.

Task 1.0 Project Management Plan

Task 2.0 Thermodynamic Cycle Modeling: A detailed thermodynamic model of an 80,000 btu per hour heating capacity single-effect ammonia-water absorption heat pump with condensing combustion was developed using the Engineering Equation Solver (EES) software platform. Mass, species and energy conservation equations were applied to each component of the model and provided temperature, pressure, flow rate and concentration data. Heat exchanger effectiveness, overall conductance, and closest approach temperatures were used where appropriate. The resulting state points and heat exchanger performance parameters were then used to design the prototype components in Task 3 and provide estimated system performance over the range of anticipated ambient and water temperatures.

Task 3.0 Heat Exchanger and Combustion System Design: Heat exchangers for the nominal 80,000 btu hr^{-1} heating capacity were designed using the design state points from Task 2.0 and previously developed models. The heat exchangers were designed to utilize standard materials that are well suited for automated fabrication. An air coupled evaporator model was developed specifically for designing the ambient coil. A condensing heat exchanger (CHX) was designed in addition to the main loop components and helped improve the overall combustion efficiency. The design of a nominal 50,000 btu hr^{-1} pre-mix combustion system was performed with both modeling and experiments performed to assess heat transfer, CO and NOx production.

Task 4.0 Solution Pump Design and Testing: A scaled up version of a low cost residential heating capacity solution pump was designed and tested. Performance, reliability and projected cost were evaluated. The pump was fabricated and tested to characterize pumping efficiency, pump starting ability, amp draw, noise and other factors. Modifications to the pump, based on the test results, were implemented.

Task 5.0 Breadboard Prototype Fabrication: A breadboard was fabricated to allow for the evaluation of component and system level performance. Individual components were fabricated and/or purchased. Components were installed on the facility that allowed for evaluation at a range of operating conditions.

Task 6.0 Heat Pump Breadboard Testing: The heat pump was tested and allowed for performance evaluation and determination of operational characteristics. Limitations were identified and design changes were made based on performance of the breadboard.

Task 7.0 Condensing Heat Exchanger Testing: A condensing heat exchanger was designed and evaluated to allow for improved combustion efficiency. The performance of the component and operational characteristics were determined with component testing and testing as part of the packaged units.

Task 8.0 Packaged Prototype Design & Fabrication: Two packaged heat pump systems with a nominal size of 80,000 btu hr^{-1} were designed and fabricated, and were representative of a commercial product in size and function. The auxiliary components and sub-systems were acquired from commercial vendors. In addition a control algorithm with integrated safety systems was developed.

Task 9.0 Packaged Prototype System Preliminary Testing: Testing of the Alpha 1 Packaged Prototype was performed to verify operation, optimize the refrigerant/absorbent charge and confirm start-up and operation. Iterative optimization of control algorithms, start-up routines, and performance was performed using the Alpha 2 Packaged Prototype.

Task 10 Environmental Chamber Testing: GTI conducted 3rd party environmental testing of the Alpha 1 Packaged Prototype at ambient temperatures of 47, 32, 17 and -13°F.

Task 11 Building Energy Simulation, Multiple Climates and Building Types: The energy and utility cost savings of the heat pump system were compared to representative high efficiency and minimum efficiency gas options. A simulation test matrix was developed that included building types, climate zones and representative cities with a focus on single-family residences. Climate zones ranged from Mixed-Humid (4A) to Very Cold (7A).

Task 12 Final Review: Review performance, cost and market potential against project goals.

Task 13 Final Project Report: Results, findings, conclusions and recommendations for future work were documented in the Final Project Report.

3.0 Task 2: Thermodynamic Cycle Modeling

Development and optimization of the target cycle model was a critical initial task, as all other project tasks are based on the target cycle model and the ultimate performance, efficiency, parasitic power, manufacturing cost and reliability are heavily tied to the choices made during cycle modeling. Cycle modeling was completed using commercially available software, Engineering Equation Solver (EES), along with specialty absorption specific sub-routines developed by SMTI personnel over the past 20 years.

A detailed cycle model was developed and allowed for parametric analysis of key parameters, ambient performance sweeps, and system details such as the condensing heat exchanger, evaporator air flow and heat exchanger overall conductance UAs. An initial set of state points at 47^{o}F ambient was "locked" and set as the "baseline" cycle. A parametric analysis of key cycle state points and heat exchanger sizes was completed, with the results analyzed against their impact on performance and projected cost/reliability. A description of some key findings is presented below.

The weak solution (WS) temperature exiting the desorber impacts cycle COP, the size (cost) and parasitic power requirement of the solution pump, size of the absorber (HCA) and solution heat exchanger (SHX), and reliability (corrosion potential in desorber). Cycle COP and strong solution flow rate (pump size/power) vs WS temperature are shown in Figure 3, while HCA/SHX size (UA) is shown in Figure 4. The vertical black lines represent the value used in the "baseline" cycle. As WS temperature increases, the strong solution flow decreases, as well as the cycle COP. Both the HCA and SHX decrease in size as WS temperature increases. Generally, the HCA is one of the most expensive heat exchangers in the system, so minimizing the HCA is very important. However, corrosion potential in the desorber increases with increasing temperature, especially above 300°F. Based on these results, 270°F was selected as the "optimum" WS temperature.

This same type of analysis was repeated for the hydronic flow split between the HCA and Condenser, the effectiveness (size) of SHX and Refrigerant Heat Exchanger (RHX), the temperature pinch between hydronic inlet and solution outlet in HCA, the temperature pinch between ambient air and ammonia evaporator inlet and the temperature glide through the evaporator. Findings from the parametric analysis resulted in an optimized baseline cycle at 47°F ambient.

Predicted performance for the optimized system over a range of ambient temperatures (-13 to 65°F) was then completed and analyzed, with summary results shown in Figures 5 – 8. Figure 5 shows the cycle COP, gas-fired COP and gas-fired COP with parasitic electric power included (set

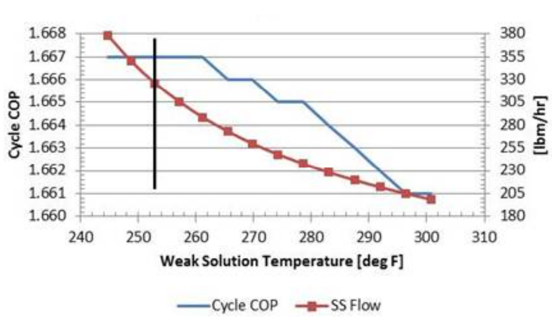

Figure 3: COP and SS flow vs. WS Temp

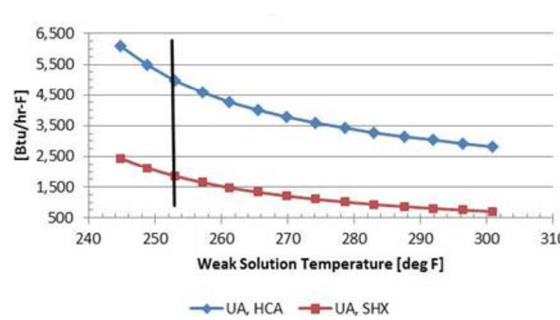

Figure 4: HCA and SHX UAs vs. WS Temp

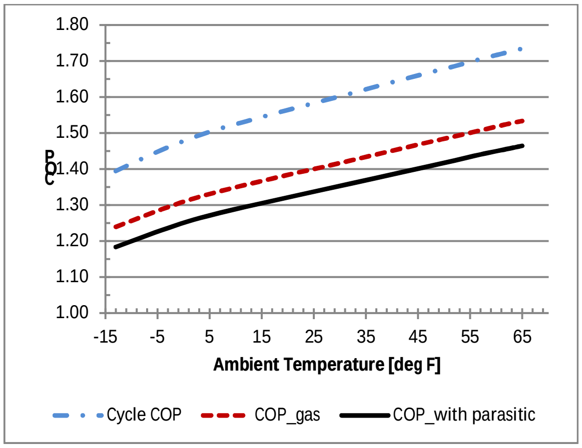

Figure 5: COP vs Ambient

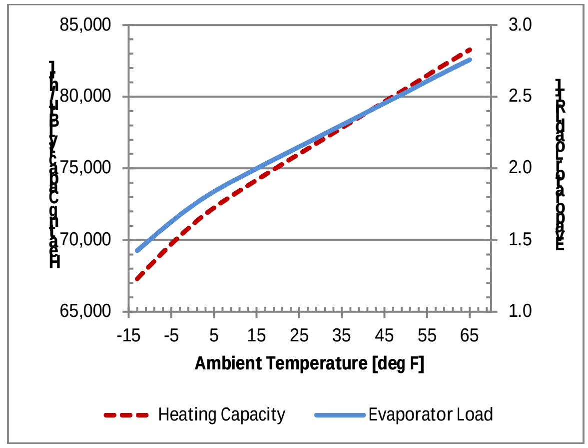

Figure 6: Heating Capacity vs Ambient

at 750 watts). Figure 6 shows the heating capacity and evaporator load, Figure 7 shows solution and ammonia concentrations, and Figure 8 shows system pressures. All plots are versus ambient temperature. The analysis was completed by locking all of the heat exchanger sizes (UAs), specifying the weak solution flow rate as a function of the differential pressure (orifice pack), a fixed evaporator superheat, a 100°F hydronic return temperature and 92% overall combustion efficiency.

The COP and capacity curves show an inflection point between 0 and 5°F, which corresponds to the rapid decrease in ammonia concentration due to the decreasing strong solution concentration. The pressure differential between the high side and low side is fairly consistent as a function of ambient, which will make system control much easier than what was experienced for the water heater product, where the differential pressure varied widely during the tank heating cycle.

Predicted vs target COP (including parasitic power) is presented in Table 1, and shows that the optimized cycle (performance and cost) matches the target (from project proposal) at all ambient temperatures except -13°F, where the COP is two points lower. A parametric analysis was completed at the -13°F ambient to evaluate cycle changes required to achieve a 1.20 COP. At -13°F, the size of the absorber, evaporator, rectifier (ammonia concentration), SHX and assumed

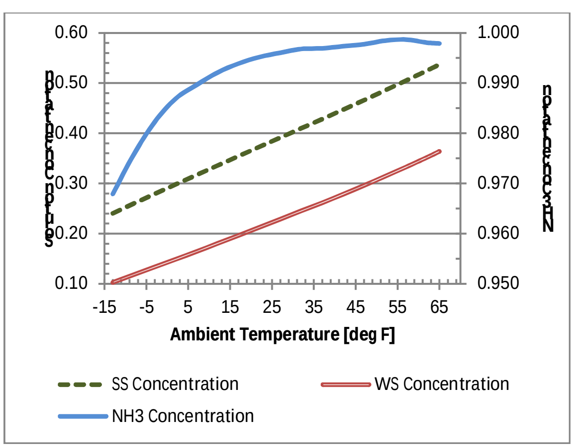

Figure 7: Concentrations vs Ambient

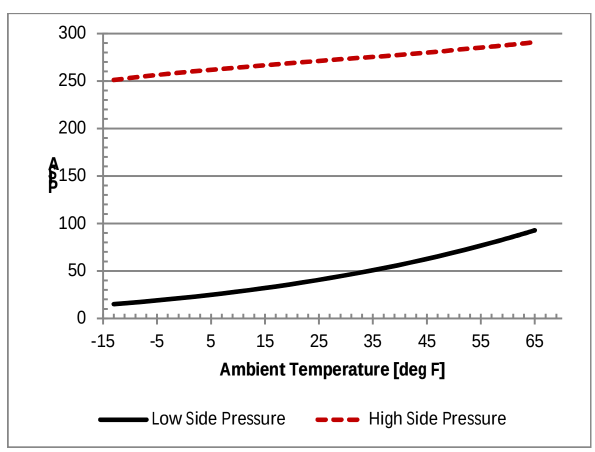

Figure 8: System Pressures vs Ambient

Table 1: Cycle Modeling Predicted vs Target				
	COP_parasitic		Heating Capacity	
Ambient	Predicted	Target	Predicted	Target
-13	1.18	1.20	67,300	68,500
17	1.31	1.31	74,600	74,700
32	1.36	1.36	77,300	77,300
47	1.41	1.40	80,000	80,000
57	1.44	---	81,850	---

parasitic power had the greatest impact. A cycle predicting a 1.20 COP was developed by increasing the absorber size by 18%, evaporator by 5%, rectifier by 6% and SHX by 12%. All of these changes increase the projected cost, with the magnitude difficult to determine prior to component design. Additionally, the size increases had a minimal impact on the predicted COP at higher ambient temperatures.

Rather than force these larger sizes and higher costs into the target cycle model, the decision was made to oversize these key heat exchangers during the design phase if the oversizing could be included at minimal incremental cost.

4.0 Task 3: Heat Exchanger and Combustion System Design

4.1 Heat exchanger design

The desorber, absorber, and condenser were all designed by scaling-up the heat and mass exchangers developed for the water heater product. This was intentionally done so that the same base materials and fabricating equipment can be used for both products if they were in production.

The augmented tube-in-tube geometry used for the water heater SHX and RHX did not scale well to the larger capacity due to limitations of available dimensions (either pressure drop or heat transfer coefficient became limitations). Therefore, SHX and RHX designs using two different augmented tube-in-tube geometries with dimensions that matched target flow rates and capacities were developed. Both versions were fabricated for breadboard testing to determine optimum design. One version utilizes a commercially available augmented inner tube, while the other utilizes an augmented tube for both the inner and outer tubes that would ultimately be produced in-house.

Evaporator design progressed in two parallel paths. SMTI and the coil vendor used to produce the water heater evaporators worked together to design an initial “traditional” tube-fin evaporator coil. The coil was bent into a U-shape to provide an overall foot-print of 36 × 36 inches. An off-the-shelf integrated axial fan/venturi was specified to provide the target evaporator air flow for this coil. SMTI also worked with fan blade/motor suppliers to specify a lower cost assembly for production models. In parallel GTI conducted the higher-level evaporator design optimization task, this started with a literature survey for the most accurate ammonia two-phase flow maps and heat transfer/pressure loss correlations. While two-phase correlations and evaporator design options are well understood for “conventional” refrigerants, very little design/engineering knowledge exists for small-scale ammonia evaporators, which is one of the highest cost components of the heat pump. These correlations were used to develop a design model that was used to conduct parametric analysis leading to an optimized (performance and cost) design.

A non-optimized evaporator coil was sized for initial breadboard testing while GTI completed detailed design and optimization.

GTI completed the evaporator design optimization model, which included four different fin profiles, return bend pressure loss, air-side pressure loss and fan power, specification of flow splits, and a relative costing factor based on total tube length, fin area, and number of return bends. The development of the model is discussed in Section 4.2.

Parametric analysis of evaporator coil designs was completed using the comprehensive design model developed by GTI. The model includes “relative cost factors” based on the amount of tube/fin material, number of return bends, etc., so each design option could be compared from a relative cost point of view. The model also takes into account the required fan power, so we ensured we did not select a design that would push our parasitic power use too high.

Two “basic” design options resulted, one a flat slab roughly 36” x 36”, and one an “L” shape roughly 56” x 24”. Both design options have “relative cost factors” about 50% of the “U” shaped alpha coil tested on the breadboard.

GTI compared initial breadboard test data to model predictions to verify the model was reasonably accurate. After model verification, SMTI had a prototype produced to verify performance in the breadboard.

4.2 Evaporator model development

An evaporator model for the GAHP was developed with the software tool Engineering Equation Solver (EES). The model was designed to have a user-friendly interface and was used by the project team members as a design and simulation tool to size new evaporators and simulate the performance of existing hardware. Including assembly and packaging, the evaporator is the most expensive GAHP component, accounting for approximately 20% of the total system cost. Additionally, it is the primary determinant of GAHP size and weight. Thus, it is critical to properly size the evaporator such to optimize cold climate performance while keeping system cost and size low.

The main difficulty in developing an evaporator model is to identify the appropriate method to estimate heat transfer to develop a well-defined problem. Because of the imperfect rectification process, a trace amount of water is carried into the evaporator creating a zeotropic mixture, a mixture with varying boiling points, resulting in a non-linear relationship between enthalpy and temperature, much different from the boiling of pure ammonia. This is caused by the fact that during the phase change process, the relative mixture fraction of ammonia/water is not equal between the vapor and liquid states and, as a result, the relative thermophysical properties (e.g. specific heat) are in constant flux. The standard method to design and simulate an evaporator becomes invalid and could lead to large errors. For zeotropic refrigerant mixtures, the nonlinearity between enthalpy and temperature leads to large change of specific heat with refrigerant temperatures.

A two-row fin-tube type evaporator as shown in Figure 9 is used to compare effectiveness-NTU method and a simple energy balance method. Ammonia-water mixture flows inside the tube as refrigerant and is arranged as cross-counter flow. Wavy fins are used and an experimental correlation is applied to calculate the air-side heat transfer coefficient [Wang et al. 1997 and empirical correlation on test data]. An average air temperature between the front and the back rows is initially assumed and iteration is conducted until the difference between the assumed temperature and calculated one is within 0.2°C. The tube-side heat transfer coefficient is calculated based on the flow regimes [Wojtan et al. 2005a and 2005b, Zurcher et al. 1999 and 2002].

Each tube is discretized into small segments as shown in Figure 10 and two methods are applied to each segment (energy balance and effectiveness-NTU). A constant heat transfer coefficient is assumed and heat transfer through the return bends is neglected. When the effectiveness-NTU method is used, the fluid properties, obtained through the built-in EES function, are evaluated at the inlet conditions of each segment. The heat transfer rate of each segment is calculated.

The sensitivity of the simulation results versus the number of segments was studied for 100 segments, 500 segments and 1000 segments for one tube. It was found that that the difference in temperature, quality and heat transfer rate is within 0.1°C, 0.001, and 0.01 kW, respectively.

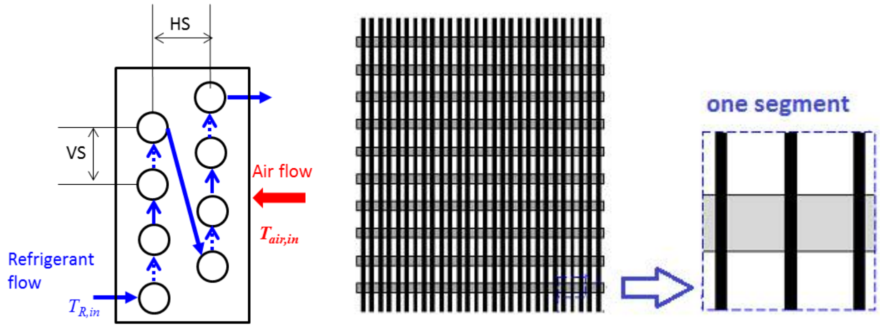

Figure 9: Flow Arrangement of the Evaporator and Discretization of the Evaporator along the Refrigerant Flow Direction

Hence, 100 segments per tube were used in the simulation and design.

The energy balance method was found to provide more accurate predictions to experimental data as compared to the effectiveness-NTU method. The effectiveness-NTU method generally over-predicted evaporator performance – the refrigerant temperature at the evaporator outlet was predicted 54% higher (i.e. 3°C higher) than test results, and the prediction on the heat transfer rate and vapor quality is approximately 5% and 4% higher, respectively. The results from the energy balance method were in better agreement with the outlet conditions of the evaporator at 9%, 3% and 2% for outlet temperature, vapor quality and heat transfer rate, respectively. More importantly, the energy balance method can simulate the trend of refrigerant temperature increase whereas the effectiveness-NTU method is not able to catch the trend, as shown in Figure 10. The inability to reasonably simulate the temperature of refrigerant mixture can lead to large errors in heat transfer rate and vapor quality calculations.

The pressure drop of the ammonia-side flowing through the evaporator is calculated based on the flow mapping for both straight tubes and the U-bends in between tubes. The pressure drop in the U-bends is calculated using the recent-developed experimental correlation and it is demonstrated to be more accurate than other models available in the public literature [Lima and Thome, 2012]. Unfortunately, the prediction on the pressure drop is much smaller than the test

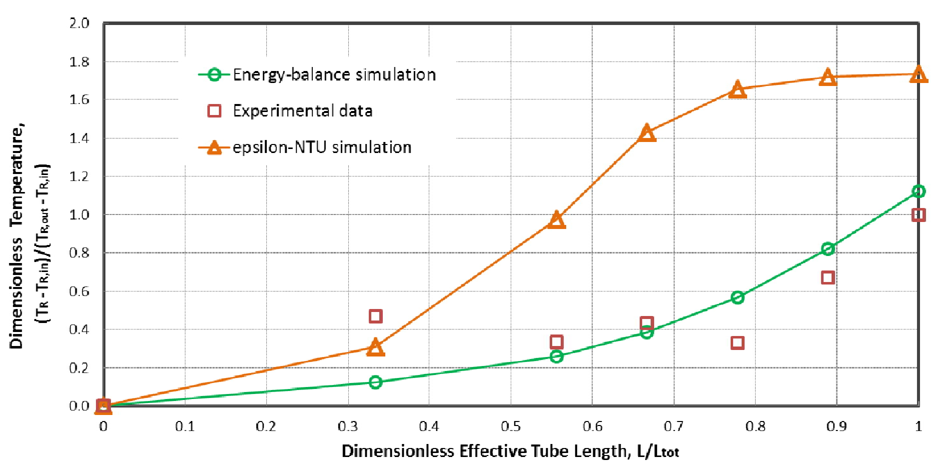

Figure 10: Refrigerant Temperature Distributions along the Tubes (Note: Effective Tube Length Is the Tube Length along the Refrigerant Flow Direction without Return Bends)

data. This difference could be resulted from the inserts into the tubes and thus a coefficient based on test data was used to characterize the pressure drop. With this coefficient, the difference in pressure drop was approximately within 10% for over 80% of the test data.

<u>Model Enhancements: CFD Analysis of Air Flow through an Evaporator:</u> The EES model is a one-dimensional simulation that assumes even air-side velocity distribution. An analysis was performed to quantify near-wall effects of air velocity distribution using Computational Fluid Dynamics (CFD) to investigate this assumption. The results from the CFD analysis were imported into EES model to evaluate the impact of the flow distribution on heat transfer of the evaporator.

The heat exchanger coil and airflow were modeled using the ANSYS FLUENT software package (v15). The airflow within the coil is modeled as a 3-dimensional porous medium, this eliminates the need to directly model the tube/coil geometries, thus limiting the quantity of computational cells required to capture the full domain. To reduce the computational effort, half of the evaporator is simulated along a plain of symmetry, thus any “swirling” effects of the evaporator fan are neglected.

The model results were compared with the test data taken at SMTI. The entire frontal area of the evaporator was divided into 13 sub-areas in the horizontal direction and 4 sub-areas in the vertical direction. The air velocity is measured at the grids and simulated in the CFD model at the identical location. Part of the model verification is shown in Figure 11. The CFD model was determined to predict the airflow field with better agreement in the center of the evaporator and some difference at the bottom ranging from 0.02 m/s to 0.04 m/s.

The CFD result of air velocity field is shown in Figure 12 as an example. The fan is mounted on the top of the evaporator and thus the airflow is drawn through the coil from the outer surface to the inner surface. The location of the fan has significant impact on the airflow – non-uniformed flow around the bending of the coil and much higher air velocity in the upper portion of the coil as comparing to the bottom. When the distance becomes large, the velocity difference in the coil surface becomes more distinct.

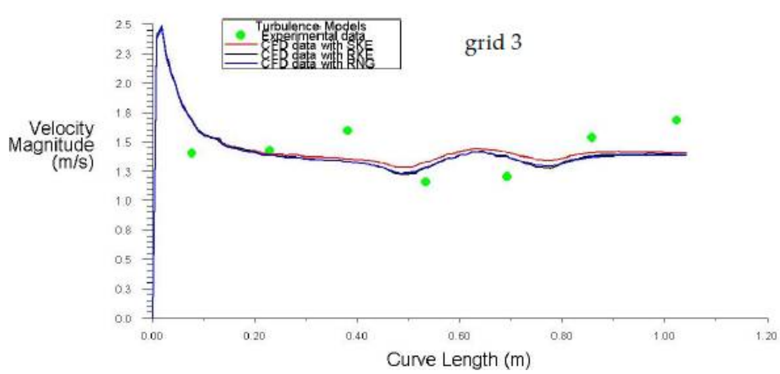

Figure 11: Comparison between CFD Results (Lines) With Test Data (Dots)

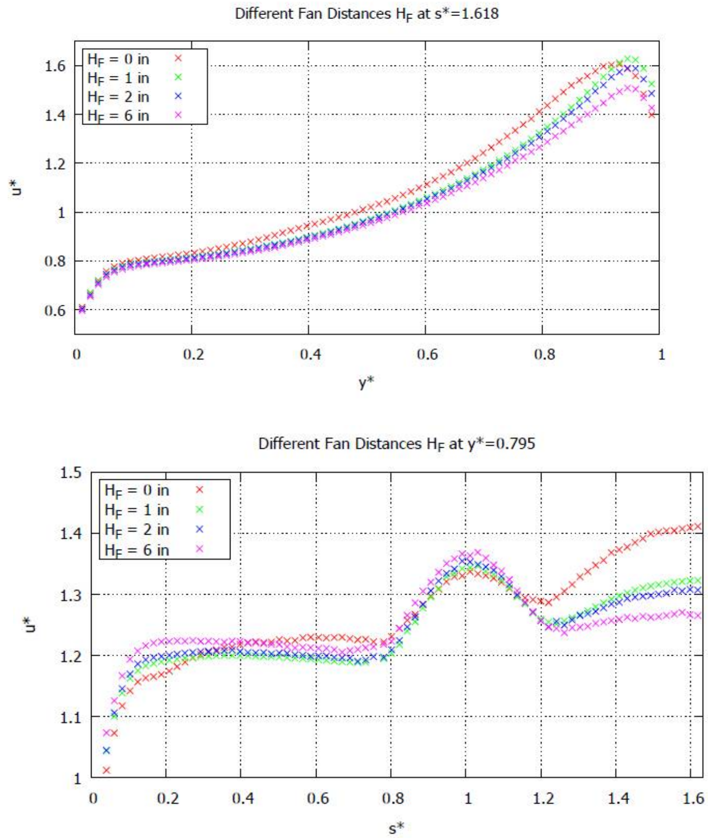

Figure 12: Comparison of Small (Top) and Large (Bottom) Distance Between the Fan and the Coil

The CFD data were used to derive a correlation as an input to the EES model. The correlation is to capture the uneven airflow field as a function of coil geometry and frontal location. The correlation is used in the EES model. An example of the results is shown in Figure 13. Furthermore, the heat load is higher for the first flow path than the second flow path (labeled as FP2 in the Figure 13).

The analysis demonstrates that the uneven airflow, for the expected ranges in local superficial

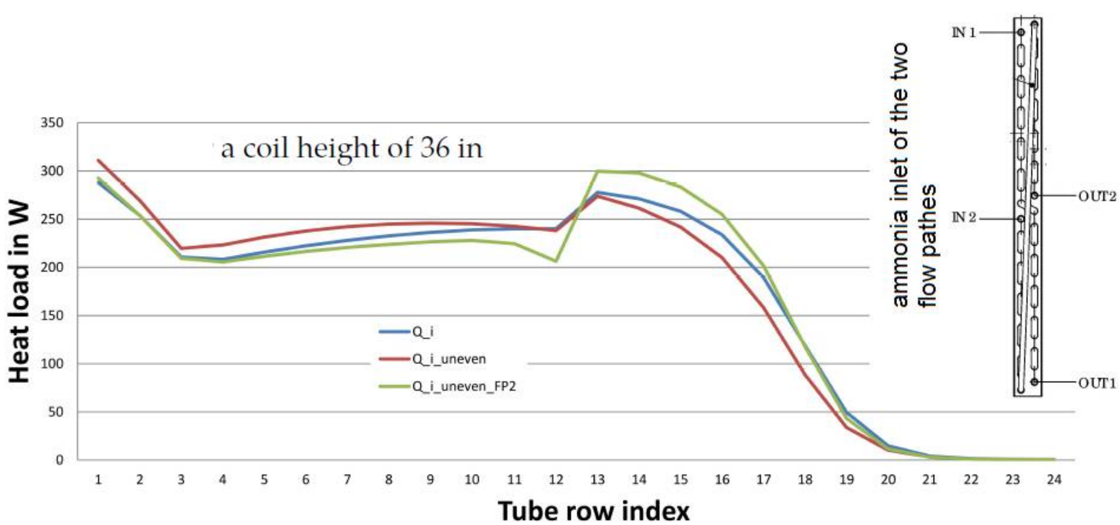

Figure 13: Heat Load of an Evaporator with a Height of 36” With Even and Uneven Airflow Fields

velocities, has a small impact on the evaporator performance for the range of geometries under this study. Further information on this comprehensive analysis can be found in the thesis by Friese (2015).

4.3 Combustion system design

Using lessons learned for the GHPWH investigation, a brief CFD modeling study to assess the proof-of-concept of the scaled-up cylindrical burner design was performed, using the same modeling methodology employed in the GHPWH development. The “SMTI Long” design for the GAHPWH application was scaled up with several constraints applied. Beginning from initial desorber dimensions provided by SMTI, a baseline CFD model was built using ANSYS FLUENT (v14). A baseline model was developed and operated, with the same model assumptions as previously used [Garrabrant, 2013].

From the initial simulation cases, the CO emission problem was shown to be intensified. This increase is not entirely unexpected, as, despite having similar porting and superficial velocities, the chamber radius has not completely scaled with the increased firing rate. In other words, the need to increase port rows and density maintains superficial velocities and port loading for the increased firing rate, but it increases the total flow rates, decreasing the average chamber residence time for post-combustion gases. This leads to lifted flames, approximated by peaks of CO in Figure 14.

To determine the validity of these results, indicating a significant increase in CO emissions for the scaled-up GAHP burner concept, two modeling assumptions were examined: the assumed pressure drop across the burner ports/mesh that would tend to affect flame distribution, and the assumed reduced-order combustion reaction mechanism.

Burner pressure drop was investigated and it was determined that it had a limited effect on the 75% open area case investigated, with very high CO emissions predicted, and therefore it was not the likely issue. The combustion model was then investigated using an alternative global finite-rate chemical mechanisms for simulation of methane combustion. Using the work of Bibrzycki and Poinsot [Bibrzycki, 2010], two alternate two-step mechanisms and one four step mechanism

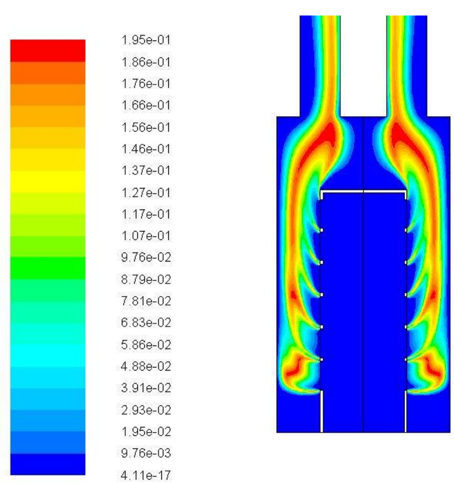

Figure 14: Baseline GHP CFD Model Showing Contours of CO Mole Fraction (dry, air free)

were evaluated for the baseline case assuming a baseline pressure drop of 3.0" WC. It was determined that the combustion model assumption makes a significant difference in the estimation of CO emissions, particularly due to the inclusion of the reversible "water gas shift" reaction in the four step mechanism (last reaction step). As it is most conservative with the estimate of CO emissions, consistent with prior experience in the GHPWH development program, the second finite rate two-step global mechanism "2 Step B" from the reference was used for subsequent analysis of chamber geometries.

Combustion Chamber Sizing Analysis

Beginning with the baseline burner and chamber geometry with a small burner diameter, and the combustion model assumptions of the "2 Step B" mechanism, the impact of geometry variation was quantified. Results for varying the chamber height and diameter are shown in Table 2 (in the table, s is greater than r and x is greater than w).

The gap between the burner outer diameter and the chamber inner diameter is an important dimension for post-flame CO oxidation. Shortening this gap, by increasing the burner outer diameter for the baseline chamber geometry, results in a significant increase in CO emission for a large OD versus a medium or small OD.

The difference between the medium and large OD burner in CO emissions appears to be purely based upon greater heat loss to the periphery due to this shorter "quenching distance" for post-flame gases. While there are not major differences in flow patterns, the average temperature of post-flame gases is lower in the large OD burner case.

A cone shaped burner design was also evaluated as an alternative to the cylindrical shape as it (a) orients the post flame gases with more of a vertical trajectory, increasing gas residence time prior to quenching on the chamber perimeter wall and (b) may increase the available mesh surface area for a given burner height. Following baseline CFD modeling, SMTI elected to build the alpha desorber with a Y height combustion chamber, to alleviate this post-flame CO oxidation issue. For this taller combustion chamber, a truncated cone burner was modeled.

In addition to modeling the baseline performance of the conical burner in its standard chamber, parametric analysis was performed on increasing the chamber diameter and height yielding similar results to the cylindrical burner. Shown in Figure 15, the baseline case has a 31% reduction in CO emissions from the baseline cylindrical burner, in large part due to the taller combustion chamber. Increasing the chamber diameter for a fixed height yields the greatest emission reduction by almost an order of magnitude, whereas increasing the chamber height and

Table 2: Variation of Chamber Geometry for Small Baseline Burner

Case	Chamber Diameter	Chamber Height	Percent Change from Baseline	
			CO Emissions	Pressure Drop
Baseline	r	w	0%	0%
Parametric Runs	r	x	-55%	-4%
	s	w	35%	-5%
	s	x	-14%	-7%

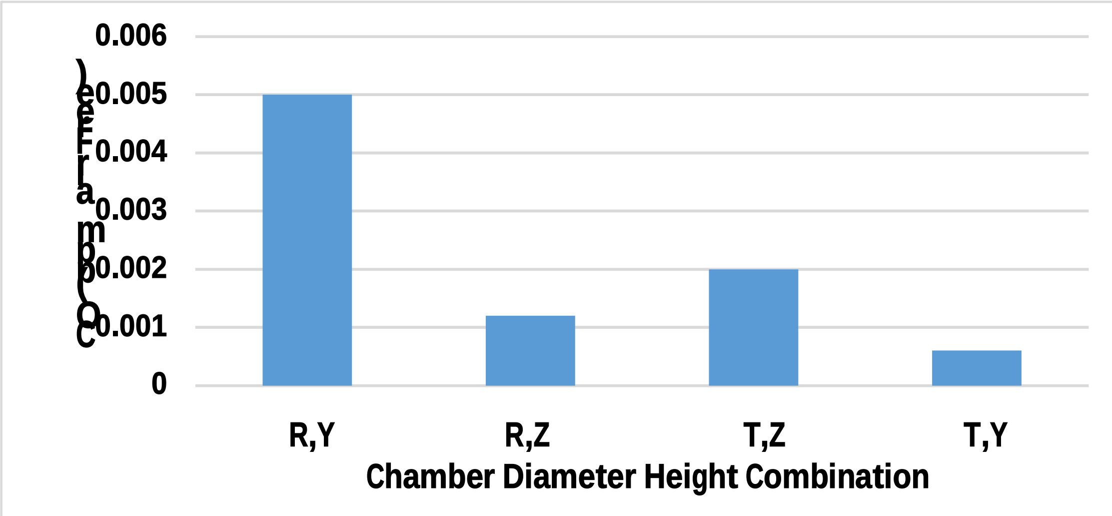

Figure 15: Impact of Chamber Height and Diameter on Conical Burner

diameter together does not yield an additional emission reduction benefit.

In comparing the baseline cylindrical vs. conical burners, beyond the increased height of the combustion chamber more significant emission reductions were expected due to the larger active surface area. Visualizing CO formation, shown in Figure 16, reveals where the cylindrical burner generates CO due to strained flames all along the burner elevation, the majority of CO generated by the conical burner is at the bottom of the burner mesh.

The CO generated at the burner bottom is due to excessive strain rates, from a stagnant toroidal circulation pattern. This may cause the oxidation of CO to be mixing-limited locally, as local temperatures are adequate for oxidation. Investigating the local turbulent kinetic energy (TKE),

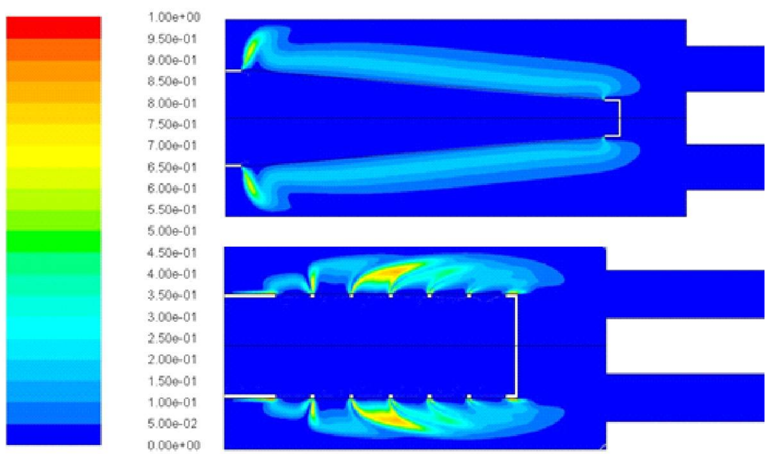

Figure 16 Contours of CO Concentration (ppm air free) for Baseline Conical & Cylindrical Burners

the reaction rates of methane to CO and CO to CO2, and superficial velocity along the mesh showed that this is the likely cause. As velocities are low, as is the local TKE (a measure of turbulence), the rates of reactions 1 and 2 are at their lowest near the bottom of the mesh. To address this, two changes were tested: reducing volume of the stagnant area below the mesh and using an internal insert to alleviate the maldistribution of fuel/air mixture along the mesh elevation.

The first method of limiting the excess CO formation at the chamber bottom was to eliminate the 'dead' volume below the mesh bottom. With two versions, with a flat bottom flush to the mesh bottom and with curved chamber bottom to further limit dead volume, the baseline conical burner is simulated. The step, curved or flat bottoms were found to offer no benefit in emission reductions.

Alternatively, conical inserts were simulated of various heights to be inserted within the burner suspended from the upper cap. With previous simulation during the GHPWH development, this was shown to improve the velocity distribution along the mesh. Figure 17 shows that this method could present viable CO emission reductions. Examining the contours of CO concentration for the tallest conical insert in Figure 18, the distribution improvement over Figure 16 is apparent.

Like the conical burner design, similarly inspired by the combustion system from a prior GAHP development, lowering the burner relative to the combustion chamber with a highly insulated boundary is simulated. Returning to the cylindrical design, with a W tall combustion chamber, the burner flange is lowered from its baseline position by 50% and 100% of the burner height. The surrounding wall below the desorber combustion chamber flange, either half or the full height of the burner, is simulated as adiabatic. Multiple orders of magnitude emission reductions are observed in Figure 19.

In summary, several design modifications were evaluated for their opportunity to reduce CO emissions if experimentally verified to be excessive. In order of predicted effectiveness: an added sub-chamber adiabatic section, conical inserts, and a larger chamber diameter will each contribute to reduced CO emission rates if necessary. These tools can be deployed

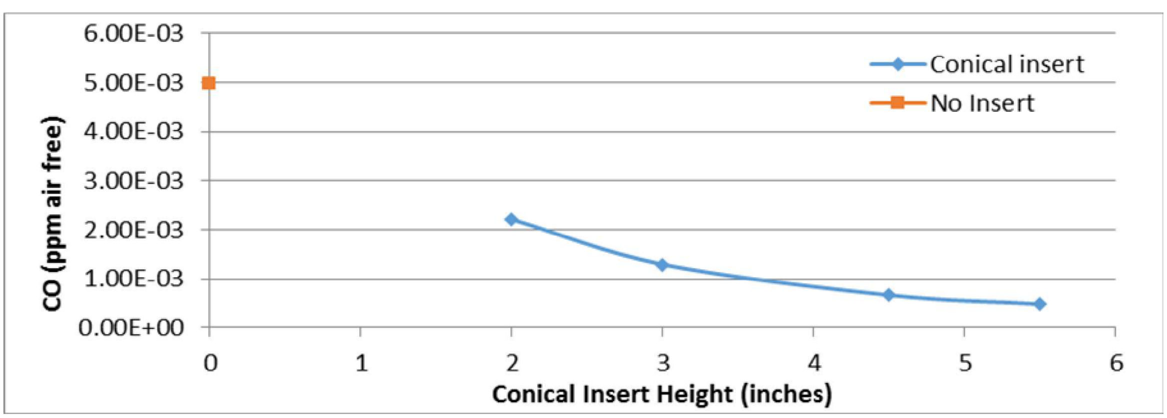

Figure 17: CO emissions for Conical Burner with Conical Inserts of Various Heights

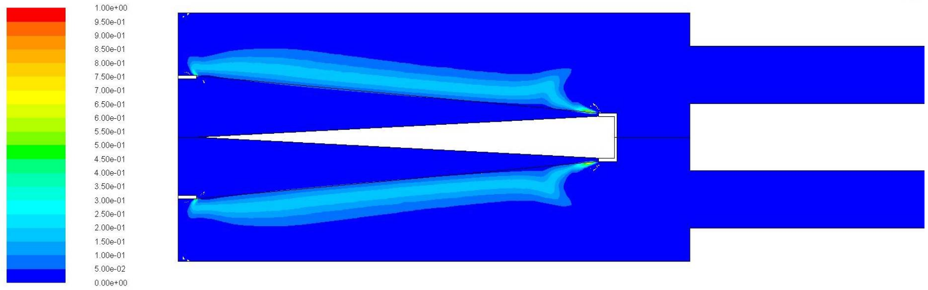

Figure 18: Contours of CO Concentration (ppm air free) for Conical Burner with 5.5" Conical Insert

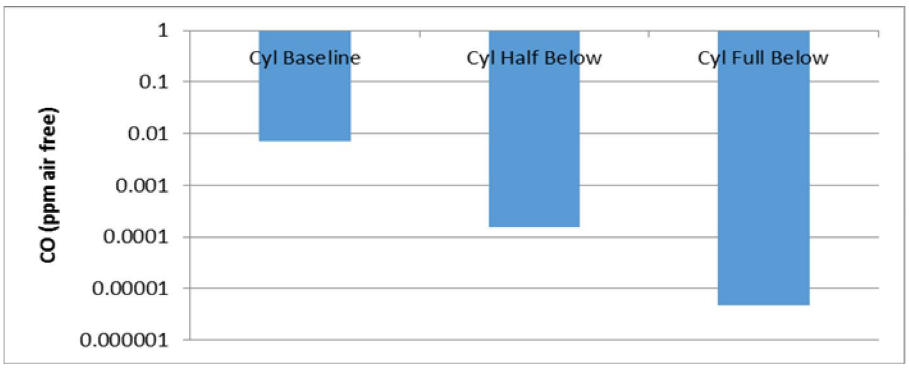

Figure 19: CO Emissions (air free) for Addition of Sub-chamber Adiabatic Section

experimentally on an as needed basis.

Combustion System Testing

A mock-desorber was fabricated and shipped by SMTI to be used as a water-cooled test chamber for GAHP burners at GTI. While the simulated heat sink temperature of the boiler NH_3/H_2O mixture at ~300°F is not recreated, a tankless water heater is used to preheat water entering the desorber at 140°F. All testing used the same blower/gas valve/mixer system (hereafter "gas train"), which with through integration with a standard PWM signal generator provided suitable combustion system control over the balance of burner testing.

In addition to stable combustion over the initial target modulation range of 3:1, the two primary emission targets are CO emissions at or below 50 ppm (air free) and at or below 14 ng NO_x/J output. Concerning the former, prior simulations suggest that the CO emission target may be challenging to meet, however noting that the predominant ANSI requirement for gas-fired residential equipment is not to exceed 400 ppm CO (air free) for *indoor equipment*. Concerning the latter, this NO_x requirement is based on the South Coast Air Quality Management District (SCAQMD) Rule 1146.2 for boilers and process heaters (including tankless water heaters) with rated inputs of less than 2MMBtu/hr. An important aspect of this target is that technologies like the GAHP with rated efficiencies of greater than a COP of 1.0, the allowable NO_x target can be higher than for conventional combustion equipment. As the estimated COP is anticipated to be 1.4 or above, this NO_x limit actually is less stringent due to an efficiency greater than 1.0. As a guide for this effort, the effect that COP has on this 14 ng/J NO_x limitation in ppm NO_x at 3% O_2 is as shown in Figure 20. For a 1.4 nominal COP at 47°F, the GAHP performance target, the NO_x emission rate should be less than 32 ppm at 3% O_2.

Fabricated Conical/Cylindrical Burners

Two classes of burners were evaluated: those with woven or knitted fiber mesh flame holders and those with a sintered fiber mat, the latter generally having a higher pressure drop, though less expensive to manufacture. Initial testing began with the former, using inexpensive perforated plate material and knitted fiber mats to assemble cylindrical and conical burners. Once assembled and welded, two mesh burners, one cylindrical and one conical, were shipped to SMTI for parallel testing.

The cone and cylindrical burners were fired in open air and were found to have a significant vertical distribution problem, owing in large part to the narrow inlet port from the mixer upstream. Brief experimentation found that the use of baffles and/or a smaller perforated tube with packing within the burner assembly could achieve better vertical fuel/air distribution. However ultimately this was not a long-term solution, as the orifice on the burner mating flange was opened up to 1.0", with which open air testing confirmed acceptable vertical distribution for firing within the desorber.

When firing the cylindrical burner within the desorber achieving a stable operating point at the target firing rate of approximately 55,000 Btu/hr, it was found that: The burner performed best and most stably with significant back pressure on the system. When operating with significant back pressure and a stable flame, the flue gas outlet temperature was excessively high, 550°F or greater. To address the short residence time of flue gases, GTI made and used flue baffles (similar to those initially tested in the GHPWH and found to be unnecessary).

Flue baffle length and placement were varied, finding that fewer than 14 baffles (all flue tubes) does not lower flue gases below 500°F and that using 14 baffles for the length of the flue tubes (flush with the transition from the combustion chamber) extracts too much heat, with exiting flue gas temperatures of less than 150°F. The flue inserts necessary to provide back pressure for stable combustion and for increased heat transfer to reduce exit flue temperatures from 550°F+

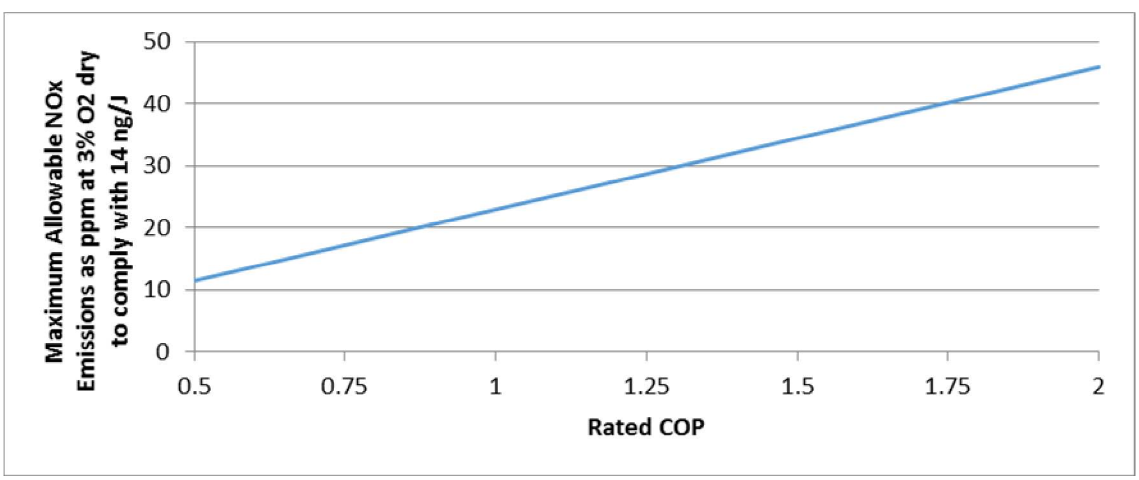

Figure 20: SCAQMD Rule 1146.2 NO_x Requirement vs. COP

down to the desired range of 250°F-350°F, were determined to be 20” long.

Results indicated that CO emissions are significantly lower than predicted by prior CFD for the cylindrical burner, though not ideal. CO emission rates were generally between 100 and 200 ppm air free, suggesting that minor improvements are required to reach targets. The discrepancy between these results and the CFD results are due in large part to the fact that the CFD modeling did not impose back pressure on the burners, found to be required for stable firing. Also, that the heat extraction from the chamber is believed to be overestimated within the model.

For these fabricated cylindrical and conical burners, with woven fiber mesh flame holders, once back pressure and inserts were applied to address flame stability and internal fuel/air distribution was addressed, the performance looks acceptable for these designs. High-fire flue gas temperatures were in the desired range of 300-350°F and CO and NO_x emissions are quite good for all cases, acceptable for this first generation design (Figures 21-23). Minor adjustments with fuel/air distribution via the perforated plate (eliminating the packing/inserts) and operating under design conditions with 350°F NH_3/H_2O heat sink versus the 140°F-160°F water jacket may yield nominal reductions in CO emissions.

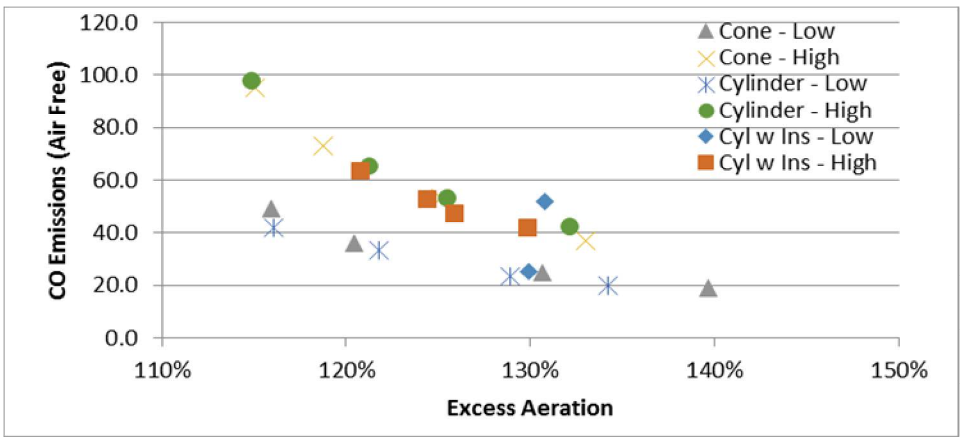

Figure 21: CO Emissions for Cone & Cylinder Burners with Loose Packing and Cylinder with Insert

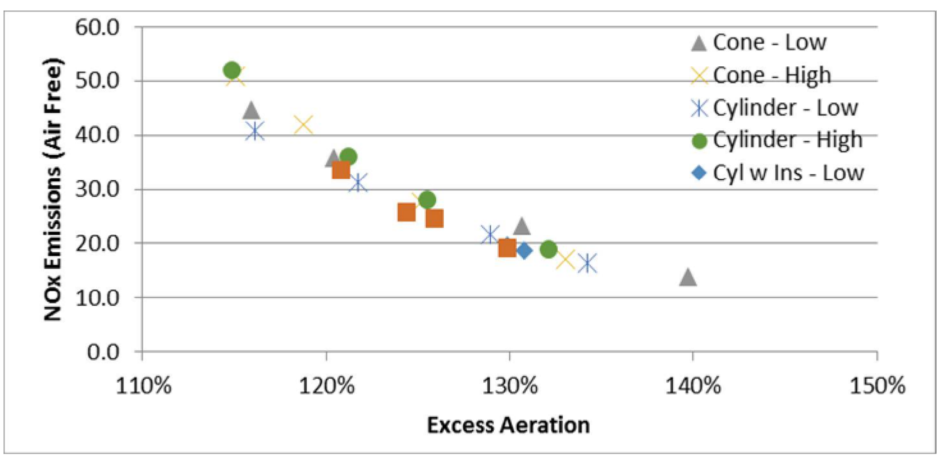

Figure 22: NO_x Emissions for Cone & Cylinder Burners with Loose Packing and Cylinder with Insert

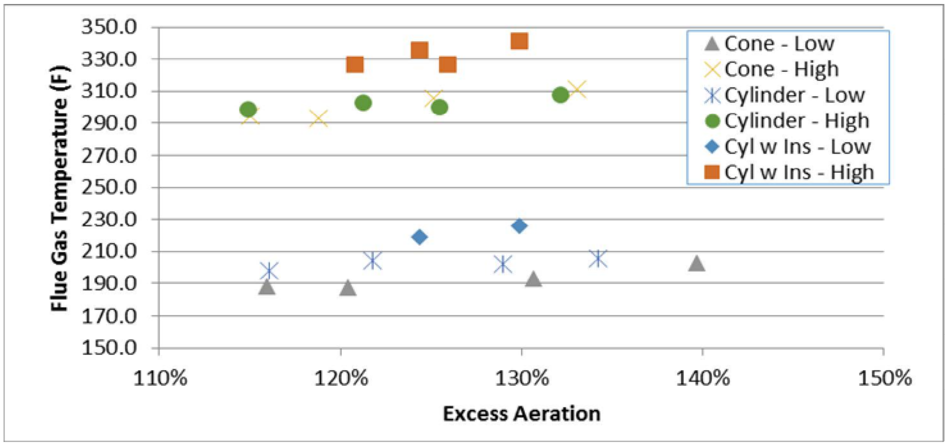

Figure 23: Exit Flue Temperatures for Cone & Cylinder Burners with Loose Packing and Cylinder with Insert

Solicited Burner Designs

Using the cylindrical design as a template, whose performance is comparable to the conical burner and will be more readily manufactured, burners were solicited from four vendors: A, B, C, and D, with the latter two using a sintered metal fiber mat and the others using a woven fiber mesh. Open air testing of all burners demonstrated successful ignition, however the Vendor B and initial Vendor C samples would not operate at the target 55,000 Btu/hr input stably. Vendor A and Vendor D burners showed excellent distribution over the range of modulation 3:1. For the Vendor B burner, with a smaller O.D. than other burners, firing into the desorber under a range of conditions at 100%/50% input, fuel rich to fuel lean with 0 to 7" WC back pressure, and ignition was not sustained. A larger diameter Vendor B burner was later tested by SMTI that met all performance and emissions targets.

Comparing burners in Figure 24, they each have acceptable performance, with NO_x and CO emission rates within a narrow range. The Vendor C burner does appear to have best low-end performance where CO emissions do not increase with higher excess aeration, indicating better turndown control. By contrast, the Vendor A and Vendor D burners have partial lift-off at high excess air/low fire resulting in a spike in CO emissions. Recalling that compliance with SCAQMD requires an emission rate of approximately 32 ppm at 3% O_2, converting this to 0% O_2 (air free) yields 37 ppm NO_x, which all three burners meet without issue. Similarly, with moderate excess aeration all burners meet the 50 ppm CO emission target as well. Several solicited burners were tested without desorber flue inserts, which demonstrated increased flame stability in comparison to prior fabricated burners, due to reduced open port area on perforated plates, however exiting flue gases were exceedingly hot above the 300-350°F target, thus inserts were deemed to be necessary.

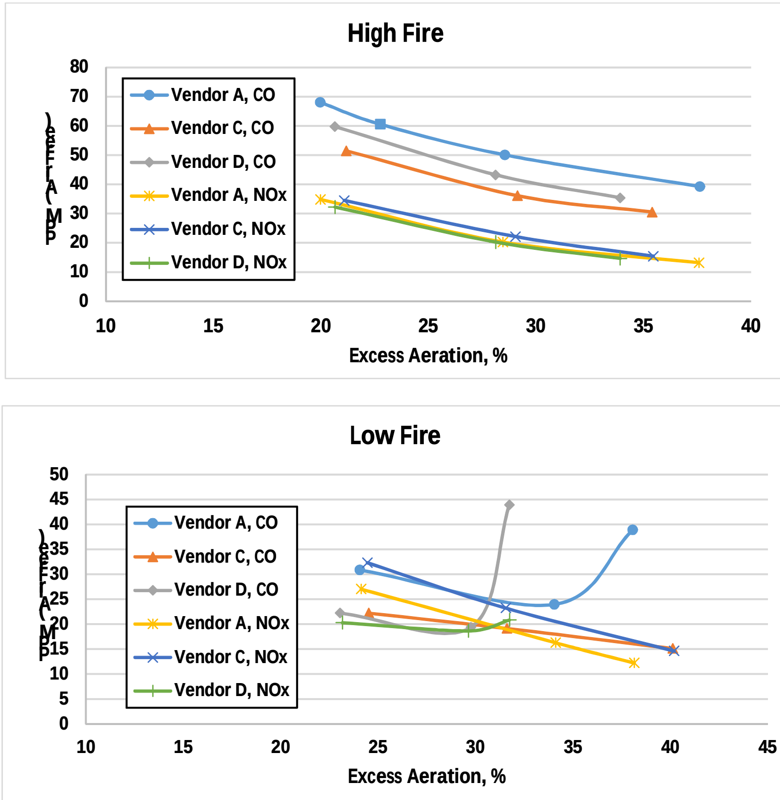

Figure 24: Comparing Emissions at High Fire (Top) and Low Fire (Bottom)

<u>Burner testing as part of the GAHP:</u>

Several burners, combustion blowers and modulating gas valves were evaluated at SMTI in parallel to GTI's work as part of the breadboard and packaged prototype phases. SMTI's experience was similar to GTI's for many of the early burner prototypes. A larger burner supplied by Vendor B performed better than all previous units but still required manual manipulation to start the unit. Analysis indicated choked flow upstream of the burner, and when corrected, very good ignition, steady-state and modulation performance was obtained.

Alpha 2 was investigated using burners from Vendor B and C in combination with two different blower systems (1 and 2). Results from this investigation are presented in Figure 25. The plot shows that the burner and blower combinations produce similar amounts of CO and NOx for the excess air range investigated. Modulation of the blower systems was also investigated and it was determined that the second blower system allowed for improved control during modulation and better low ambient temperature performance.

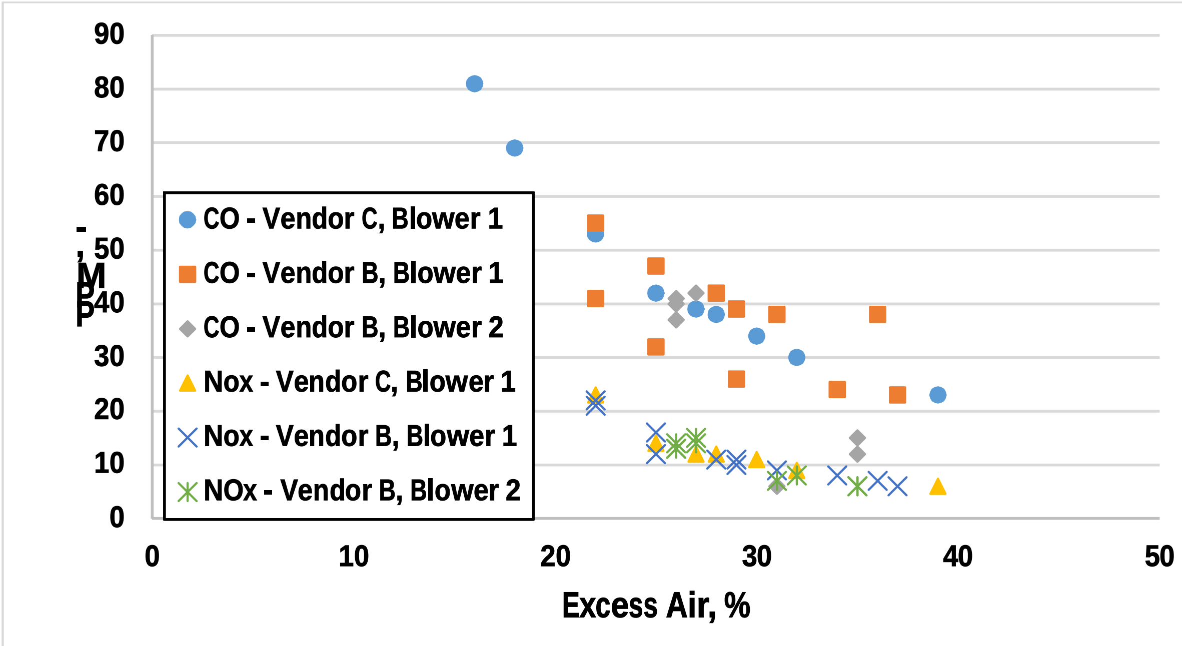

Figure 25: Comparing burner and blower combinations used on Alpha 2

5.0 Task 4: Solution Pump Design and Testing

Several design options were evaluated for scaling the low-cost single-piston pump developed for the water heater product up by a factor of 10 for the space heating application. Options included 1, 2 and 3 piston designs, inline and opposed, stroke length and RPM. Manufacturability, cost, bearing load/size, reliability and motor horsepower were considerations. The concept selected is an opposed 2-piston pump using the same stroke and lower speed as the smaller version. The opposed design provides a positive return so we ensure good performance at very low ambient temperatures (very low inlet pressure,) and provides 10X the flow with only a 5X motor HP increase. Keeping the same stroke allows us to transfer elastomer seal reliability data from our small pump life tests to this design. The lower speed provides some built in overhead for a future higher capacity model using the same pump.

An Alpha Solution Pump was fabricated, assembled and tested (Figure 26). Bench testing of the alpha Solution Pump was completed.

The pump was tested using water at an inlet pressure of 70 psig over a range of pump speeds (495 – 666 RPM) and outlet pressures (200 – 350 psig). The pump ran smoothly and quietly. Figure 27 shows the volumetric pump efficiency (measured volumetric flow divided by the maximum theoretical), as a function of the differential pressure. Efficiency decreased with increasing differential pressure as expected, as “slip” flow past the pistons increases with differential pressure. At a given differential pressure, efficiency increased with speed, as there is less time for the slip flow to occur.

To check the pump’s ability to pull a vacuum, the inlet of the pump was connected to a hose sitting in a bucket of water about 30” below the pump. The pump was able to self-prime and develop 250 psi of outlet pressure while pulling water from the bucket. The pump was also able to produce about 10 psi outlet pressure when pumping air only.

Our design volumetric flow rate is 141 in^3 min^{-1} and we measured 156 in^3 min^{-1} at 473 RPM, so we should be able to operate the pump at about 500 RPM. Design differential pressure is 215 psi, with a target volumetric efficiency of 90%.

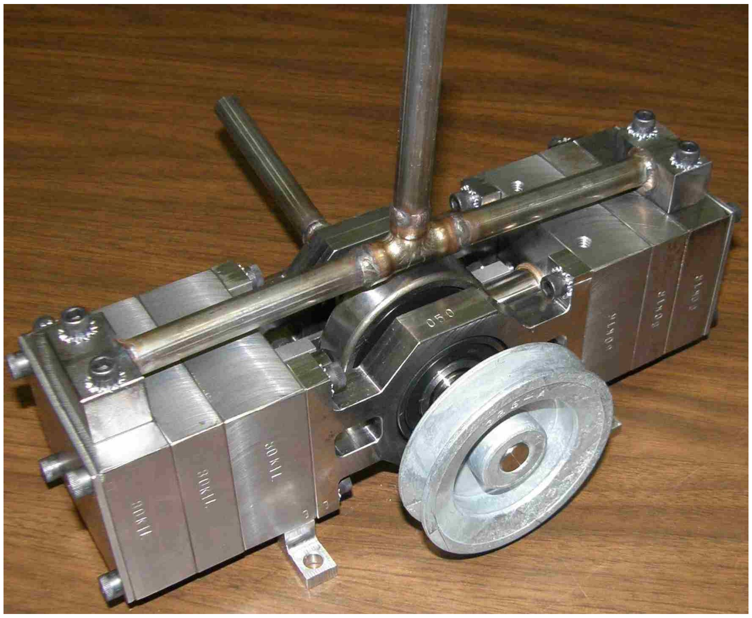

Figure 26: Alpha Prototype Solution Pump

The solution pump provided very good performance during breadboard and packaged unit testing. Slight modifications were made to the pumps throughout the project to improve pumping efficiency, improve reliability and reduce noise.

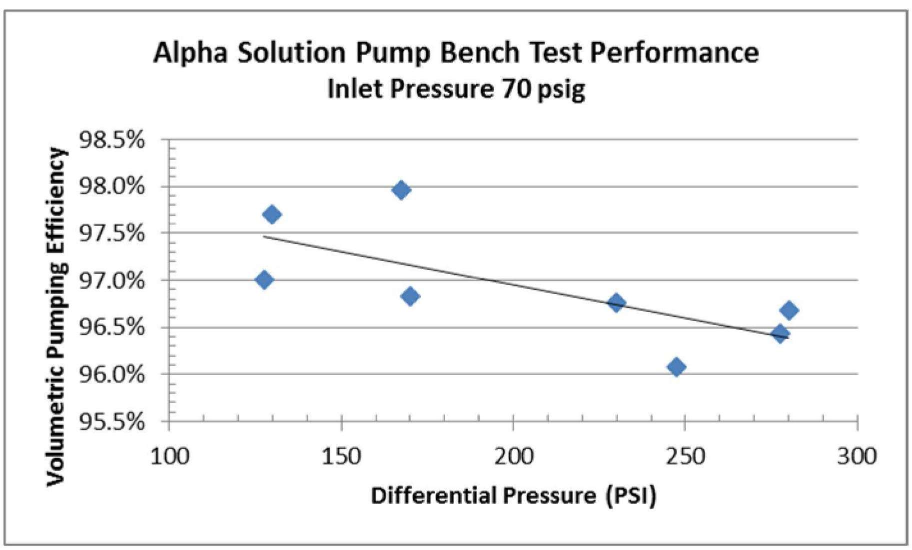

Figure 27: Alpha Solution Pump Bench Testing (water)

6.0 Task 5: Breadboard Prototype Fabrication

Heat exchangers and supporting components necessary for breadboard testing were fabricated and received. Modifications to the SMTI test room (to increase ambient cooling and heat pump heat rejection capacities) were performed. The components were installed in the breadboard test facility (Fig. 28) in preparation for breadboard testing. The test facility includes pressure, temperature and flow rate measurements to allow for accurate analysis of system performance.

7.0 Task 6: Heat Pump Breadboard Testing

Breadboard testing was performed over the course of several months. The first several weeks were focused on establishing the correct charge of ammonia and water, debugging instrumentation and the control scheme, getting the combustion system set-up properly, and a general understanding of how the system performed. After completion of this initial shake-down test period, data point testing was initiated to evaluate component and system performance. An iterative approach was taken where a limiting component or components were identified. These components were then replaced with a redesigned or modified component. Evaluation of these component changes and the resulting change in performance was the performed. At the end of breadboard testing, system performance was approaching the design conditions. Performance was also investigated over a range of ambient and return water temperatures. The following is a discussion of the each component and the overall system.

Absorber: Initial testing showed that this component was slightly underperforming. A second round of testing confirmed the component was operating below design at around 85% of target capacity. Adjustments to the design internals were performed, a Rev2 unit was fabricated, and overall system performance was improved.

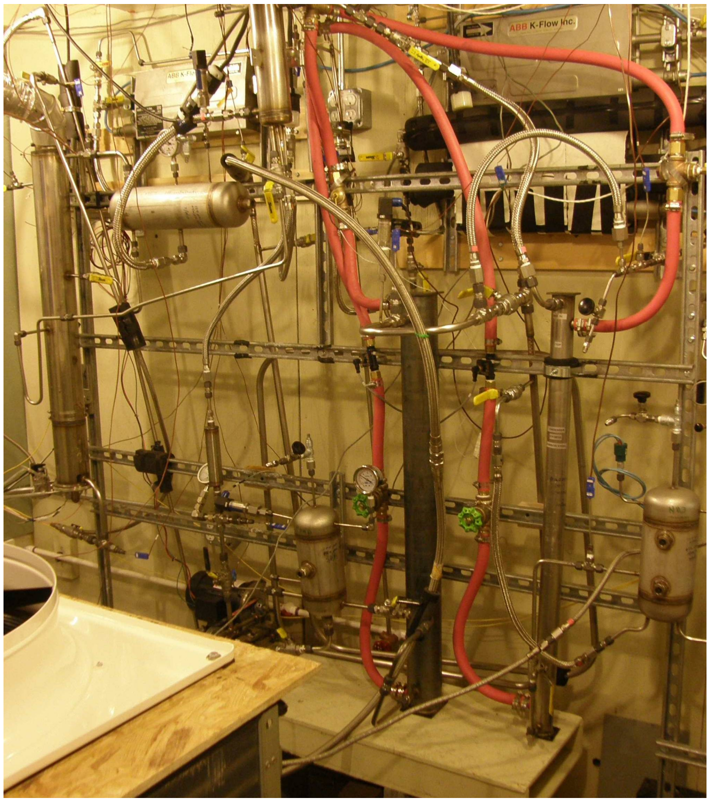

Figure 28: Breadboard Heat Pump System

Condenser: Initial testing showed that this component was performing at or above target performance levels. Performance near design continued throughout testing of the breadboard system.

Desorber: Initial testing showed that this component was performing at or above target performance levels. Further testing showed that the alpha desorber appeared to be generating micron-scale solution droplets, too small to be "knocked-down" in the Rectifier and that these droplets were reducing the ammonia purity in the refrigerant loop. A Beta Desorber (Rev2) was designed where the internals of the Beta Desorber are "more open" than the Alpha, reducing the vapor velocity at the vapor-solution separation points. The Alpha design was more aggressive (as far as vapor velocity is concerned) than our HPWH design (which does not have this issue), so the Beta Desorber was sized to closely match the HPWH velocity profiles. Improvement was obtained with the Rev2 desorber, and the resulting test data and lessons learned were implemented into the Rev3 desorber, which provided the desired performance.

Evaporator: Initial testing showed that this component was performing at or above target performance levels but the refrigerant pressure loss through the component was higher than design (2-3 psi). A flow imbalance between the two flow circuits was discovered with on-coil measurements and the flow split geometry was modified to correct this. Profile data with the Rev3 Rectifier (higher ammonia purity) was recorded and used to evaluate evaporator performance against the design model.

A beta evaporator coil was designed and fabricated with pressure loss being closer to design. In parallel to the Rectifier evaluations (Rev4, Rev5, and Rev6), the Beta (significantly smaller) evaporator coil was performance tested. The measured UA of the Beta evaporator coil was 25-30% smaller than design.

As a note, the electronic expansion valve (EEV) provided excellent service over the entire range of operating conditions (including 3:1 modulation) and appears to be sized correctly for this unit.

Rectifier: Initial testing showed that this component was underperforming and resulted in lower than design purity refrigerant (0.985). A slight modification to the Rev1 design (Rev2) was made with minimal measured improvement. A Rev3 design was fabricated (slightly larger version of Rev2 with modified internals to improve vapor-tube heat transfer) and tested with significant performance improvement providing ammonia purities of 0.994 (target of 0.997). Rev4, Rev5, and Rev6 Rectifiers were designed to try to improve ammonia purity further. Maximizing refrigerant purity flow through the refrigerant loop is key to maximizing system COP which is why so much focus was put on getting the rectifier component to operate at design.

Refrigerant heat exchanger (RHX): Initial testing showed that this component was performing at or above target performance levels (both design options). Performance near design continued throughout testing of the breadboard system.

Solution Heat Exchanger (SHX): Initial testing showed that this component was slightly underperforming (both designs). A second round of tests showed that the component was operating about 5-7% below design. Based on these results the heat exchanger coil design was increased 5-10% for the packaged systems. A Rev2 SHX was designed and fabricated with minor design changes to improve overall system performance.

Solution Pump: During initial testing the solution pump performed well. A "squeaking" noise at steady-state conditions was noted when a small amount of vapor is entering the pump. After reviewing the design calculations, the velocity through the inlet valve (when vapor is present) is much higher than intended, and was believed to be causing the noise. The inlet valve was resized and the physical change was made on the Beta pump.

During testing, one of the outlet check valve springs failed and inspection revealed it was due to rubbing against the spring guide. The spring guide was redesigned to eliminate the rubbing and new guides were fabricated.

System Level: In the first round of testing, cycle COP for 14 full fire tests at the nominal 47°F ambient rating point ranged from 1.45 to 1.56, with a 1.48 average (90% of the target 1.65). Calculated energy loss to the ambient averaged 7% of the total input (based on an overall system energy balance). Energy loss to the ambient is typically very high for breadboard testing due to very long connecting lines, instrumentation (including mass flow meters), and the cold air velocity from the evaporator exit (at 5000+ cfm flow rate). A production unit would typically see a 2-3% ambient heat loss. The breadboard tests covered a range of water (hydronic) inlet temperatures of 100 – 120°F, ambient temperatures of 26 – 67°F, and burner firing rates of 18,575 – 56,000 Btu/hr. With the majority of tests conducted at nominal conditions of 101/47/54,000.

In the next iteration of testing steady-state cycle COP at nominal conditions and Rectifier Rev3 tested averaged 1.50 (91% of target 1.65). Ambient heat loss (calculated by energy balance and typically high on a breadboard system) averaged 5%, which projects the COP to 1.55 – 1.57 in a packaged design.

Overall cycle performance improved with the next iteration, with cycle COP increasing from an average of 1.50 to 1.55 (94% of target 1.65) at the design conditions.

With a new absorber, desorber, SHX and rectifier, testing at the design condition (47°F ambient, 100°F hydronic return) was completed, resulting in a cycle COP of 1.60 (97% of target 1.65) at the target hydronic flow rate (8 gpm), and 1.64 (99% of target) at an elevated hydronic flow rate of 10.6 gpm.

The elevated hydronic flow test was conducted to provide insight into the absorber performance, by forcing all of the excess flow through the absorber in order to achieve our target (ammonia-side) exit temperature. The resulting 0.04 increase in cycle COP shows that a small additional increase in absorber performance will ultimately allow the overall performance goals to be reached.

Parametric testing was completed (ambient and hydronic return temperatures) at the standard 8 gpm hydronic flow rate, with the results shown in Figure 29.

Measured trends as a function of hydronic temperature closely match that predicted by cycle modelling at 47 F ambient, as well as at 32 and 17 F. The difference between measured and target increased as the ambient temperature decreased, is primarily due to increasing heat losses to the ambient, which was supported by the energy balance calculation for each test. In a packaged unit, the “hot” sealed system heat exchangers are protected from the cold air flow exiting the evaporator fan, in addition to having much shorter line lengths and no instrumentation. There was also a small amount of frost build-up on the evaporator coil during the 5 and 17°F tests.

Modulation: Breadboard testing then switched focus to modulation testing with all of the heat exchangers and support component designs finalized. Modulation (load matching) is very important for this product for two reasons:

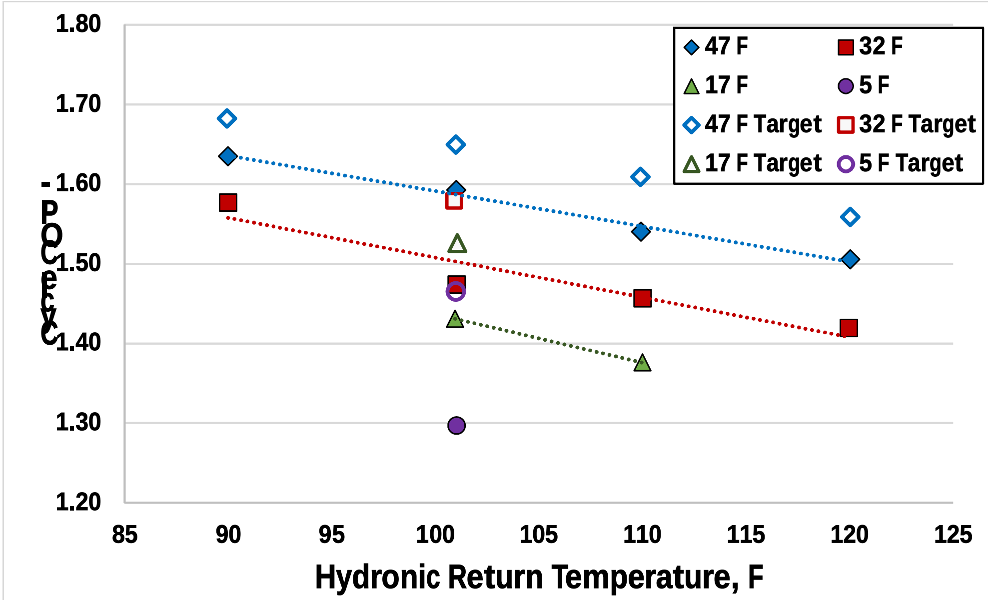

Figure 29: Cycle COP vs. Ambient and Hydronic Return Temperature

- Residential space heating equipment is normally sized for the coldest anticipated ambient temperature, such that the equipment is technically over-sized 95% of its operating hours.
- Absorption systems do not like to be turned on and off and tend to have higher cycling losses than furnaces or boilers. The ability for the heat pump to modulate down and match the load to minimize on-off cycles is important for overall seasonal efficiency optimization.

The stated project goal was at least 2:1 modulation, but the preferred target was 3:1. Unlike direct-fired furnaces or boilers, modulation of an absorption heat pump is more difficult than simply reducing the firing rate and maintaining good combustion. Working fluid movement from the high pressure side to the low pressure side is governed by the differential pressure, the fluid path is tortuous and often involves 2-phase flow. Eventually, these flows will become unstable once the energy input rate drops below a certain value. Extra piping lengths and instrumentation (mass flow meters) used in our breadboard test cell makes this problem more difficult.

Testing consisted of initially achieving steady state conditions at the full input rate, then reducing the firing rate via the variable speed combustion blower. The modulating gas valve-venturi maintained the fuel-air mixture constant.

Seven steady-state data sets were recorded covering modulation ranges from 1:1 to 4.7:1 (Figure 30). In all cases, the system ran even, without cycling or instabilities. At 4.7:1, the EEV was bouncing off of the closed position trying to maintain evaporator superheat due to the very low ammonia flow, but was not at that point of causing instabilities or performance degradation.

Cycle COP (47°F ambient, 101°F hydronic return temperature) remained above 1.52 for all tests, higher than we anticipated for a breadboard system due to the ambient heat loss becoming a higher percentage as the input rate is reduced (Figure 30). *This suggested that the packaged*

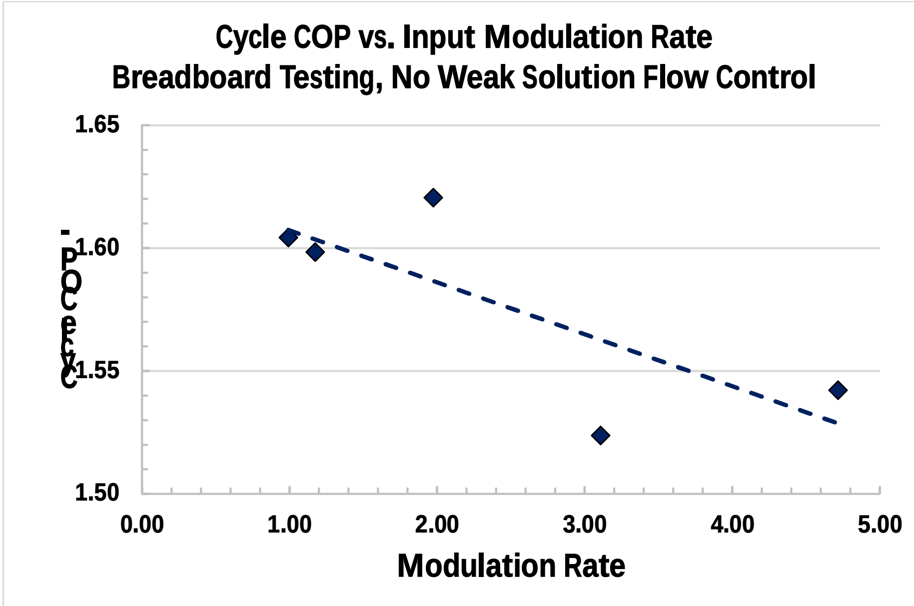

Figure 30: Cycle COP versus the input modulation rate

prototype would be able to achieve at least 4:1 modulation without significant performance degradation.

At 2:1 and 3:1 modulation, the weak solution flow rate was changed to simulate weak solution flow control, which can be used to minimize COP losses as the input rate decreases. At 2:1 modulation, reducing WS flow had a slight negative impact on COP, while at 3:1 it had a slight (1%) positive impact on COP. Based on the results, WS flow control will not be required to maintain high COPs when modulating.

8.0 Task 7: Condensing Heat Exchanger Testing

AO Smith performed testing on two prototype condensing heat exchangers (CHX), both shell-and-tube style designs. Testing was completed at the most demanding operating point for the CHX, which is at -13^{o}F ambient. The first prototype achieved a flue gas exit temperature of 110-111^{o}F (109^{o}F target). The second prototype achieved a flue gas exit temperature of 106^{o}F, with a very low 0.4" water pressure loss on the flue gas side (Table 3).

AO Smith also tested a RevB design that provided performance exceeding target performance and was used in the packaged prototypes. AO Smith built and tested a RevC design, for the purpose of determining the lowest cost size that will provide the target performance.

Table 3: Condensing Heat Exchanger Rev2 Results

	Design Conditions	Test Conditions	
Firing Rate	54,300 Btu/hr	54,837 Btu/hr	54,000 Btu/hr
Excess Air	4.63% O2 (125% max)	4.8% O2	4.55% O2
Hydronic Flow Rate	8 gpm	8 gpm	8 gpm
Hydronic Return Temperature	100°F	100°F	100°F
Water Side Pressure Drop	1-2 psi	0.66 psi	
Flue Gas Inlet	356°F	358.2°F	361.3°F
Flue Gas Outlet	109°F	105.8°F	105.9°F
Flue Side Pressure Drop	2 in wc	0.4 in wc	

9.0 Tasks 8: Packaged Prototype Design & Fabrication

Based on Breadboard test data, modifications were made to the SHX and Absorber for the Packaged Prototype. The physical layout of the packaged prototype is shown in Figure 31. The evaporator coil for the packaged prototype was sized using the calibrated GTI evaporator design model. The physical size was an approximate 50-50 compromise between the Alpha and Beta coils. The Alpha 1 solution pump was tested on the pump test stand prior to assembly into the prototype, with a measured volumetric efficiency of 88% or above at all pressures. The Alpha prototype overall dimensions are 38 x 47 x 44" tall.

Based on Alpha 1 test results (discussed in Section 11), the Rectifier UA for Alpha 2 was increased 10% and an alternate condenser to refrigerant storage tank plumbing arrangement was developed.

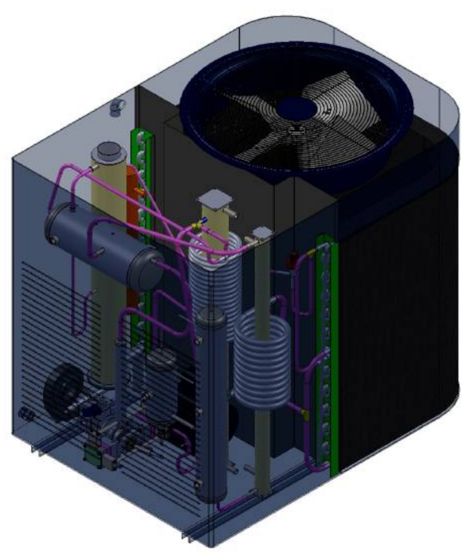

Figure 31: Packaged 80 kbth GAHP Alpha Prototype

10.0 Task 9: Packaged Prototype Preliminary Testing

Alpha 1:

Steady state tests were completed at ambient temperatures ranging from -1 to 56°F, hydronic return temperatures ranging from 80 to 125°F, hydronic supply temperatures ranging from 92 to 142° F, and gas input rates ranging from 25 to 100% of design. Measured efficiencies were within 96% of target at design conditions and 90% of target at cold ambient temperatures.

COP vs hydronic return temperature at the design 47°F ambient condition is shown in Figure 32. COP_cycle is the net heating output of the heat pump cycle divided by the net gas input (ignoring combustion losses). COP_cycle provides a measurement of how well the thermodynamic cycle is performing ignoring all other factors, with a target of 1.65 at 47°F ambient and 100°F hydronic return.

COP_gas is the gross heating output of the heat pump divided by the gross gas input. COP_gas provides a measurement of the overall system COP, ignoring parasitic power use, with a target of 1.45 at the aforementioned conditions. COP_hp includes electric power in the denominator, with a target of 1.4.

Detailed analysis of the test data, indicated that the ammonia purity exiting the rectifier was slightly below the design target (0.991 compared to 0.997) and was the primary cause for the 4% COP differential between measured and target at the 47/100°F design condition. Although it seems like a small difference, very small amounts of water vapor remaining in the refrigerant stream creates large differences in the boiling temperature/pressure in the evaporator. The extra water vapor forces the low side pressure down and, in essence, decreases the effective ambient temperature.

Part of the ammonia purity issue was a function of the solution heat exchanger (SHX), which was performing at a higher level than design (effectiveness close to 1). Long term, this is a good as COP increases with SHX effectiveness. But the high SHX performance increases the vapor temperature and water concentration of the vapor entering the rectifier, increasing its duty.

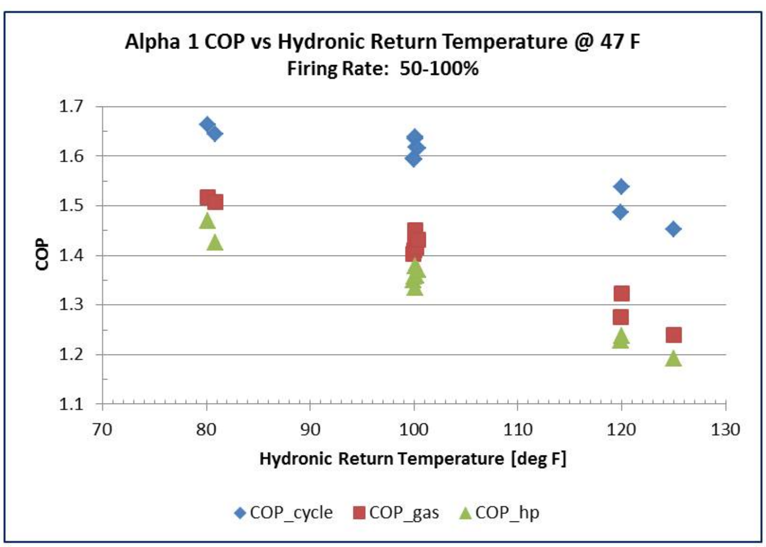

Figure 32: COP at 47°F Ambient

Since the rectifier is not designed for this higher duty, the resulting ammonia purity is less than design.

The impact of the ammonia purity issue is more pronounced at high return water temperatures and low ambient temperatures. For this reason, the measured performance is a lower percentage of target at these conditions, which can be seen in Figure 32 in the form of a bowed curve at the 120/125°F hydronic return temperature.

COP curves at 55, 32, and below 9°F are presented in Figure 33 – 35. The plots show the expected trends similar to Figure 32 (performance increases with decreased hydronic return temperature) and also that the performance increases with increasing ambient temperatures.

Figure 36 shows measured parasitic power as a function of hydronic return temperature for all ambient temperatures and gas inputs. Target parasitic power at the design condition was less than 750 watts, and we are currently well below that, averaging about 600 watts. Part of the scatter in Figure 36 is due to testing at different evaporator fan speeds. Solution pump motor power increases as the hydronic temperature increases due to the increasing high side pressure.

Testing was completed at a variety of gas input rates, with stable and efficiency operation obtained all the way down to 4:1 modulation. Modulation is an important feature for residential space heating systems to minimize on-off cycling that will reduce the effective COP. For a heat/pressure driven absorption system, the system can become unstable at very low inputs as

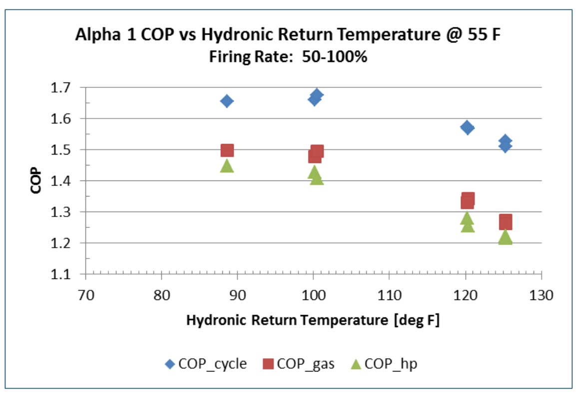

Figure 33: COP at 55°F Ambient

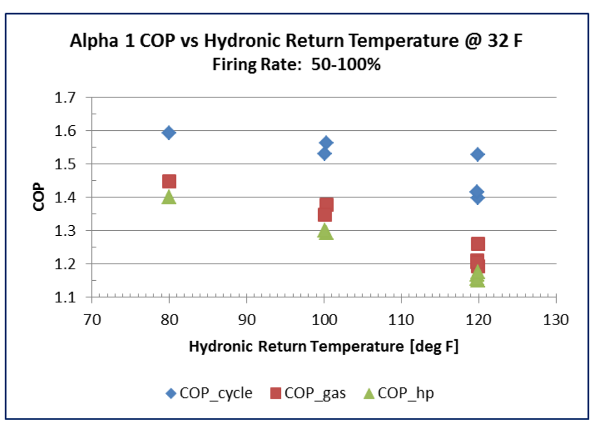

Figure 34: COP at 32°F Ambient

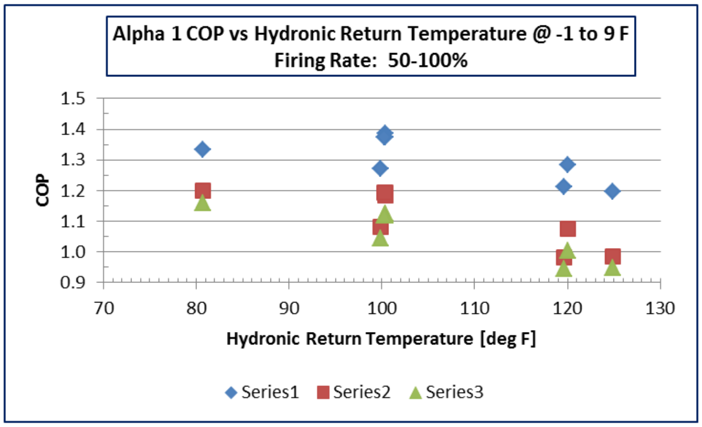

Figure 35: COP at -1 to 9°F Ambient

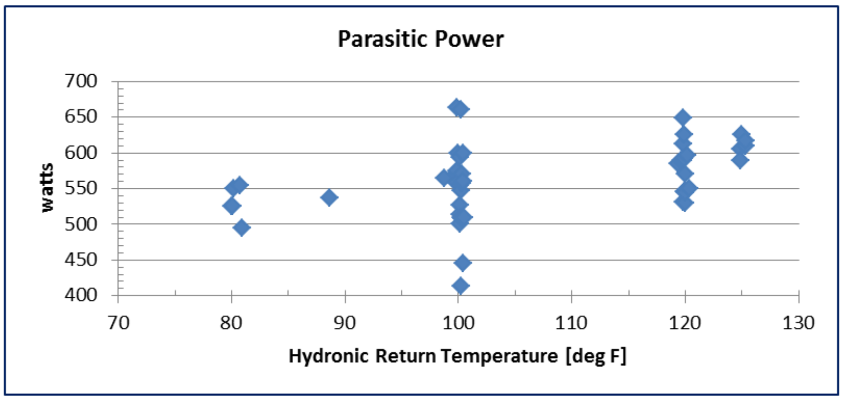

Figure 36: Parasitic Power

the circulation ratio drops substantially. Additionally, COP's often decrease significantly at low inputs if the desorber temperature decreases too far.

Figure 37 shows COP_gas as a function of the gas input percentage. COP peaked between 50 and 80% firing rates, while maintaining full-fire performance at very low inputs. Since a space heating appliance is sized for the coldest 5% ambient condition, most residential systems spend most of their life operating between 40 and 80% of capacity. As Figure 37 suggests, this matches very well with the heat pump performance and suggests real-world efficiencies may be higher than the rated.

With the completion of steady-state testing on the Alpha 1 prototype, covering a wide range of ambient/water temperatures and gas firing rates, the focus shifted to controls development and refinement for "real-world" conditions where the heat pump modulates to match the load (up to 4:1) and must switch back and forth between space and water heating modes (if installed as a combi system).

The base PLC algorithm was modified to allow automated PID control of the hydronic return (or supply) temperature by modulating the natural gas input. The actual control temperature is user-settable via a knob on the side of the heat pump control box (ie. 90 to 125° F for return temperature). Additionally, a provision was added so that the PLC could monitor external signals (on/off) from both a theoretical space heating and potable storage water heater thermostats.

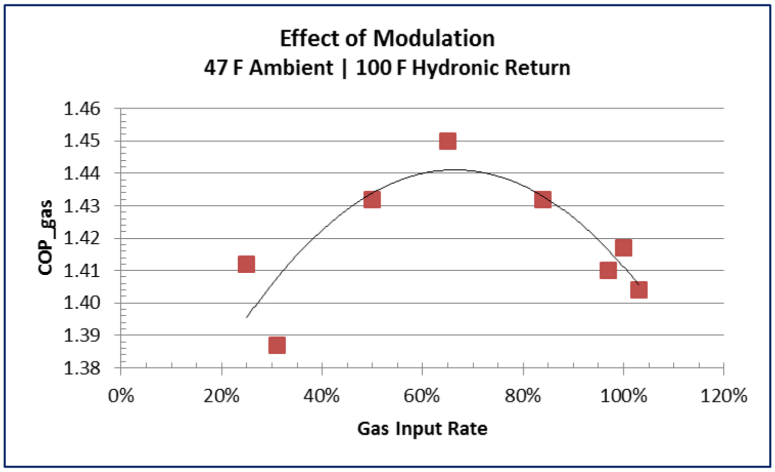

Figure 37: Effect of Modulation on COP

Using these control inputs, the heat pump is capable of matching its output to the load while maintaining a fixed hydronic temperature, and knows whether space or water heating is desired (or both at the same time).

Initial testing focused on adjusting modulation and EEV PID parameters so that the heat pump reacted "fast enough", but not so fast as to cause large temperature fluctuations. Determining the maximum rate of change the modulating gas valve could be handle while maintaining good combustion characteristics was also evaluated.

With the PID parameters established, the heat pump was exposed to a series of step changes of either the modulation set-point temperature or applied heating load to determine how the heat pump reacted, with a particular focus on system stability and safety (high pressures or high temperatures). Of particular interest were scenarios where the heat pump was operating at the maximum hydronic return temperature (125°F) and firing rate and the applied load was suddenly reduced or removed, then after a short period of time, re-applied. At the maximum hydronic temperature and firing rate, the system pressures and temperatures are also at the maximum, representing the maximum amount of stored potential energy which could create operational problems if instabilities or overshoots occur.

Based on this series of tests, the control algorithm was continuously refined such that the heat pump reacted properly to the large step changes. A few specific applied load on/off/on step change scenarios caused the high side pressure to temporarily increase above the saturation pressure and close to the high pressure switch set-point. Control logic changes did not have a significant impact on the results and, based on the measured data, it was concluded the short-term pressure increase was caused most probably by the piping arrangement between the condenser outlet and the refrigerant reservoir tank. Based on this result, this connection was modified during final assembly of the Alpha 2 prototype.

The final set of tests involved switching modes between space and water heating. Although there are many acceptable ways to handle this interaction (often determined by specific application), we chose to assume domestic hot water priority. The heat pump successfully handled moving from one mode to another, and initially turning on in either mode and switching back and forth.

Prior to shipment to GTI for verification testing, the combustion blower-gas valve combination was replaced with one from a different vendor, in order to evaluate modulation characteristics of the alternate vendor. The alternate vendor system worked very well unit the ambient temperature fell below freezing, then the gas valve could no longer maintain the desired air-fuel ratio. After discussion with the vendor (facilitated and supported by AO Smith and GTI), a slightly different model was recommended, to be evaluated in the Alpha 2 prototype.

While fully modulating combustion systems are well-known and established technology for residential and commercial boilers, they are not often used in outdoor installations. Combustion system operation in very cold weather conditions will be a point of emphasis with combustion system vendors during post-grant commercialization activities.

<u>Alpha 2:</u>

The Alpha 2 prototype is essentially identical the Alpha 1 except that is has a slightly larger and modified Rectifier design to improve ammonia purity and the piping arrangement between the condenser outlet and refrigerant reservoir tank was modified to improve high side pressure stability during sharp operating condition transients (Figure 38).

Steady state tests were completed at ambient temperatures ranging from -1 to 55°F, hydronic return temperatures ranging from 95 to 125°, hydronic supply temperatures ranging from 106 to 145°F, and gas input rates ranging from 32 to 100% of design. Measured efficiencies were within 95% of target at design conditions. Test data showed that the larger rectifier resulted in increased refrigerant ammonia purities flowing through the evaporator (0.996 purity at the design 47/100°F). However, testing showed that the gains from this improvement were offset by a reduction in performance in the absorber. Performance of the absorber was reduced as a result

Figure 38: Alpha 2 Unit installed in test room

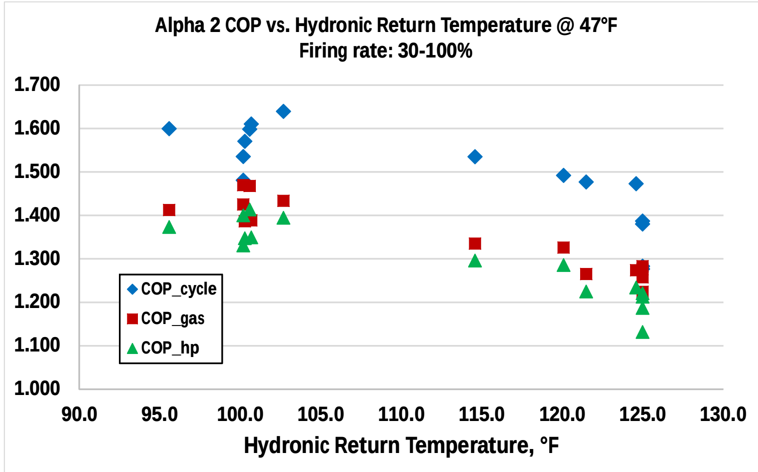

Figure 39: Alpha 2 COP at 47°F Ambient

of damage that occurred when the unit was shipped from the assembly vendor to SMTI.

COP vs hydronic return temperature at the design 47°F ambient condition is shown in Figure 39. Experimental results for Alpha 2 are similar to those reported for Alpha 1. More time was spent investigating modulation which is the cause for the vertical variation at a given hydronic supply temperature. System performance was further investigated at ambient conditions of 55, 35, and <13°F with similar results to those reported for the Alpha 1 packaged prototype.

Figure 40 shows measured parasitic power of the unit as a function of hydronic return temperature for all ambient temperatures and gas inputs. Parasitic power for all cases is well below the target of less than 750 watts, and about 50 to 100 watts below the parasitic power required for the Alpha 1 prototype. The power reduction can be attributed to changes to the fan mounting. Part of the scatter in the presented data is due to testing at different evaporator fan speeds, similar to testing of Alpha 1.

Figure 41 shows COP_gas as a function of the gas input percentage for Ambient/Hyd. Return temperatures of 47/100°F and 32/100°F. Similar to results for the Alpha 1 unit, COP peaked

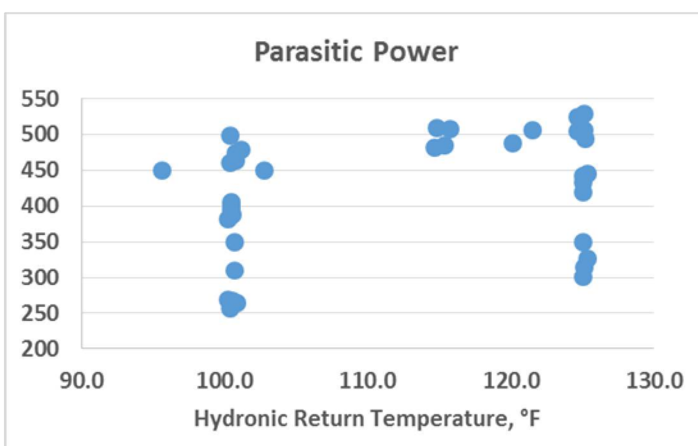

Figure 40: Alpha 2 Parasitic Power vs. Hydronic Return Temperature

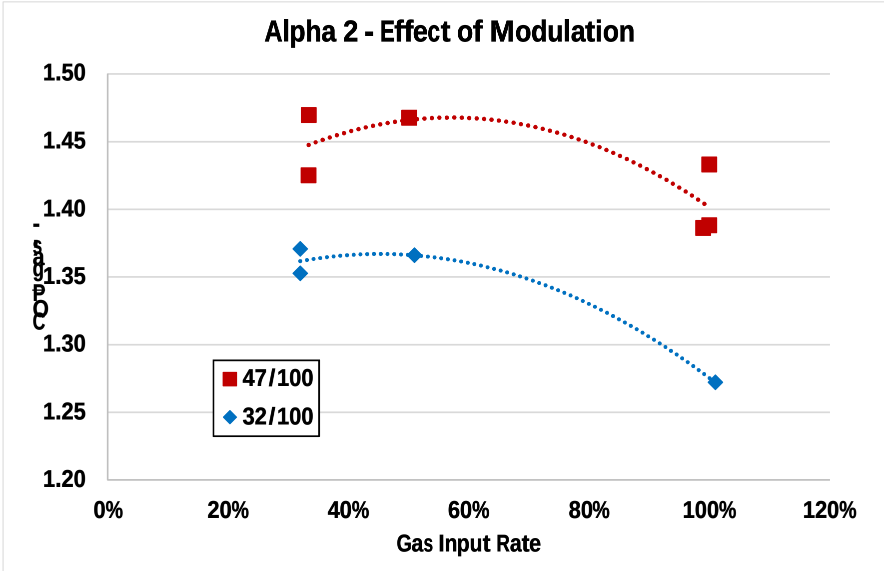

Figure 41: Alpha 2 COP_gas vs. Gas input rate

between 50 and 80% firing rate while maintaining full fire performance at low gas inputs. Operation at the 32°F ambient indicates that the peak shifts slightly to lower firing rates. This is expected based on the 47°F results and that the effective heat exchanger area will be higher for the lower firing rates. At less favorable ambient conditions, more effective area will typically result in increased performance.

Defrost methods were investigated for the very low ambient conditions where the evaporator could be coated with a layer of frost. It is important to note that when the evaporator coil of the GAHP is frosted it will continue to run without significant operational issues. Its performance will however drop to that of a condensing boiler as limited heat will be transferred in the evaporator. This is significantly different than electric heat pumps that have to shut down entirely because un-evaporated liquid slugs flowing to the compressor would shorten the life of the compressor. Control strategies were investigated that would allow the unit to continue to run while attempting to defrost the evaporator coil. Several methods were investigated and it was determined that a hot gas bypass would be required to actively defrost the evaporator coil while the unit was in operation.

The ability to achieve a 160°F hydronic supply temperature was then investigated. Operation at this supply temperature is of interest because it would allow the heap pump furnace to replace boilers in retrofit applications. If possible, this would be another potential market for this product. Modeling showed that the unit would require slight modification to the control strategy to provide the 160°F delivery temperature. Without modification, the maximum allowable pressure would have to be increased and this would result in higher material costs and a more expensive system. Implementation of the devised control strategy allowed the Alpha 2 unit to provide 160°F hydronic supply at full fire without requiring an increase in the maximum potential operating pressures. The experiments conducted on Alpha 2 showed that the heat pump could be used readily for boiler replacement retrofits.

11.0 Task 10: Environmental Chamber Testing at GTI – Alpha 1

The Alpha 1 prototype was shipped to GTI for 3rd party testing within an environmental chamber. The test plan included an array of steady state rating points, which are split into two groups:

- **ANSI Z21.40.4-1996 *Performance Testing and Rating of Gas-Fired Air Conditioning and Heat Pump Appliances*** –This test procedure, in effect today, is performed as written for steady state conditions at 47°F/35°F/17°F/7°F. The heating seasonal efficiency equivalent to an Annual Fuel Utilization Efficiency (AFUE) was calculated from this dataset.
- **Performance Mapping Steady State Tests –** Steady state tests were performed in addition to those required by the ANSI Z21.40.4 test, which covered (a) a range of hydronic return temperatures from 95°F to 120°F, (b) maximum/minimum input levels not covered by the ANSI test for various ambient conditions, (c) and an added low ambient point of -13°F. These data points were necessary to create a complete performance picture

<u>GAHP Test Setup</u>

The packaged Alpha 1 prototype was installed within GTI's Residential Environmental Chamber. As described previously, the GAHP is intended for an outdoor installation and is hydronically-coupled to the conditioned space. The GAHP was installed wholly within a simulated environmental chamber with hydronic return and supply connections running to external piping loops outside of the chamber. Chamber temperature is monitored by an array of twelve thermocouples and humidity by two relative humidity sensors, the thin-film capacitance type sensor.

Photographs of the test set-up are shown in Figure 42. For all tests, the boiler loop flow rate, the loop including the GAHP, was set at 8.0 gallons per minute (gpm) per SMTI guidance. The hydronic return temperature was set by the rate of cooling at a plate heat exchanger, defined by the flow rate and cooling water temperature of the primary loop. Steady state data points were taken when GAHP cycle, loop temperatures, and chamber environmental conditions were stable, with data recording and averaged over a period of no less than 15 minutes. Despite construction per guidance from and in the pursuit of executing the ANSI Z21.40.4 method of test, GTI's laboratories are not certified by per AHRI/GAMA requirements. *Therefore, while some reported results are from executing ANSI test procedures, they are only relevant in relative comparison to experimental data from this project.*

<u>ANSI GAHP Rating Test</u>

The ANSI Z21.40.4 method of test was developed in the 1990's to rate the emerging group of gas-fired heat pumps and A/C equipment. This ANSI test is comprised of a series of steady state rating points under static conditions, at full and partial loading, using a bin method. Data from these rating points are used in a standard calculation to generate an annualized efficiency. Comparable to the rating metric for gas furnaces and boilers, the resulting Annualized Fuel Utilization Efficiency (AFUE) is a ratio of useful heat delivered over a complete heating season to the gas consumed to drive the gas heat pump. Like furnaces, the AFUE does not include electricity consumption in the denominator. This is similar in this regard to the previously defined *COP_gas*.

Figure 42: Photos of GAHP within Chamber (L) and External Boiler/Primary Loop (R)

The primary inputs into the ANSI bin method calculation are: gross gas input, heat output to the hydronic loop, and total electric power consumed by the GAHP. These data are shown in Table 4, with the resulting COP_gas for each point. Designed to operate with a 3:1 turndown though later demonstrated to meet 4:1, the GAHP controls allow for continuous modulation, thus the tests were performed with fixed firing rates. The maximum firing target is 55,000 Btu/hr, noting that a natural derating occurs at lower ambient temperatures that are not adjusted for. “Minimum” firing is approximately 30% of max fire and “Mid/Intermediate” firing is approximately 60% of max fire. Using referenced fractional bin hours for a selected climate region, the slopes of heating capacity, balance point temperatures for each input rate, and resulting gas/electricity input rates are estimated. Selecting the climate region IV, corresponding to an outdoor design temperature of 5°F and 5,643 bin hours, and comparable to the “Cold” region in Figure 43, the results are as follows:

- **Efficiency:** AFUE = 136%
- **Seasonal Output:** 128.1 MMBtu Heating Output
- **Seasonal Consumption:** 943 Therms, 5,274 kWh

Table 4: Input/Output Data for ANSI Rating Points

Rating Point	Firing Rate (kBtu/hr)	Heat Output (kBtu/hr)	COP_Gas	Total Elec. Power Input (kW)
1	16.5	25.5	1.54	0.55
2	16.4	23.8	1.45	0.56
3	16.2	21.9	1.35	0.52
4	30.8	43.5	1.41	0.58
5	55.2	79.7	1.44	0.63
6	52.5	71.9	1.37	0.63
7	50.1	62.9	1.26	0.59

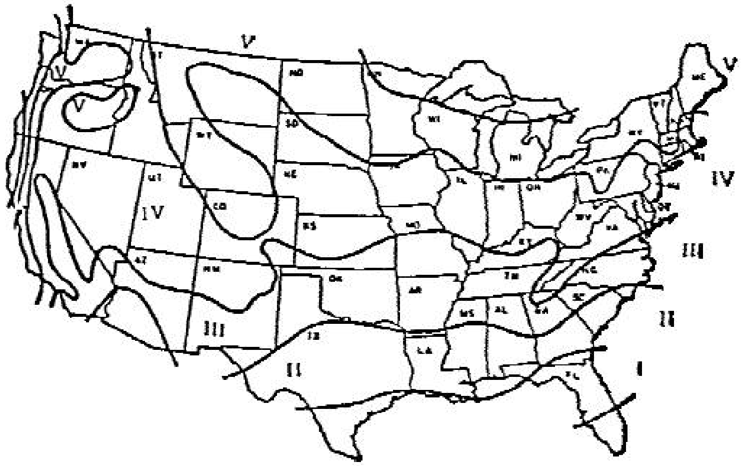

Figure 43: Climate Region Map for ANSI Z21.40.4

Additional Steady State Tests

In addition to the steady state rating points conducted for the ANSI Z21 test, GTI performed an additional 30 rating points, with some repetition of test points where necessary. These test points have the following ranges:

- **Ambient Temperature:** 47°F, 35°F, 17°F, 7°F (just ANSI point), and Sub-zero testing. As the GAHP supplemented the cooling capacity of the chamber, the sub-zero temperatures reached depend on the GAHP capacity.
- **Hydronic Return:** 95°F, 110°F, and 120°F, in some cases 90°F and 100°F are also tested.
- **Modulation:** Min./Mid./Max (30%/60%/100%) for most cases.

GAHP testing for these 37 test points, including those used in the ANSI rating, includes two important biases, the servicing of the GAHP unit and the use of propylene glycol/water as a boiler loop anti-freeze during sub-freezing testing and, in two cases, above-freezing retests.

Sub-Zero Testing

In total, the following test points were run successfully:

- Mid. Fire with ambient temperatures ranging from 0°F to -6°F, with hydronic return temperatures of 95°F and 110°F.
- Min. Fire with an ambient temperature of -6°F and a 95°F return temperature
- Max Fire with ambient temperatures ranging from -11°F to -13°F, with a 95°F return temperature.

Two issues anticipated during sub-zero testing that were not problematic were:

- **Frosting of coils** – At colder temperatures, it was expected that some frost would form on the GAHP evaporator coil. This would require cycling of the system or other means of limiting frosting as the prototype was not equipped with an automatic defrosting capability. Throughout all tests, no frosting was observed.

- **Gas valve operation** – The gas train within the GAHP tested was the Vendor 1 unit described previously in the combustion system development section. Subsequent Alpha prototypes were built using the Vendor 2 unit. Discussions with Vendor 2 indicated that the gas valve might not function at ambient temperatures below -15°C (5°F). While there was an expected "derating" of the GAHP at lower ambient temperatures, from 55,000 Btu/hr input nominal down to 48,000 Btu/hr at -13°F, there were no observed issues with the gas valve or regulators. This may be due to the Vendor 1 design, that the compartment within the GAHP stayed sufficiently warm, or some combination.

Steady State Test Results

Steady state tests are shown in Figure 44, sorting COP_Gas by ambient temperature, firing rate, and hydronic return temperatures. Overall, two important trends emerge:

1) System efficiency (output as well) are strong functions of hydronic return temperature, a 10°F increase in return can reduce COP_Gas by over 5%. However, the GAHP is not as sensitive to ambient temperature, at Max fire operating with a COP_Gas from 1.50 (47°F) to 1.17 (-13°F). By comparison, an electric ASHP will have a site-based COP of 3.57 (47°F) drop to 2.0 (-10°F) [Caneta, 2010].
2) The alpha GAHP exceeds performance targets at above-freezing ambient temperatures and is near or misses targets at sub-freezing ambient temperatures. Table 5 summarizes the most comparable points, with red text indicating those that fall below targets. The accumulation of non-condensable gases and potential for non-optimal charge volume may be responsible for this shortfall.

It should also be noted that temperature readings errors occurred for some of the low temperature testing that resulted in improper control of the refrigerant superheat. This would result in reduced heat pump performance. The 50% fire, 95°F hydronic return and 0°F ambient is believed to be one such case.

Figure 45 outlines the GAHP emissions sampled for several test points. Generally, emissions of NO_x and CO are low, particularly at Min./Mid. firing rates, at or below 60 ppm air free. For Max fire test points, the GAHP has CO emission rates that exceed that of the 50 ppm air free target, but well below that of the typical 400 ppm air free ANSI limit for domestic gas-fired equipment. As shown in Figure 46, fan power consumption is similarly a function of ambient temperature, with data shown for all test points. The balance of power consumption (controls, combustion blower, etc.) is largely insensitive to ambient conditions. Referring back to Figure 36, it is clear that the fan power is a significant user of electricity for the Alpha 1 unit at around 50%. A modification was made to the fan mounting between Alpha 1 and 2 that resulted in significant decrease in unit and fan power (Figure 40). In addition, the vertical spans on Figures 36 and 40 are a result of varying the fan speed. This would be done when the unit is operated at a reduced firing rate to reduce the parasitic draw from the fan.

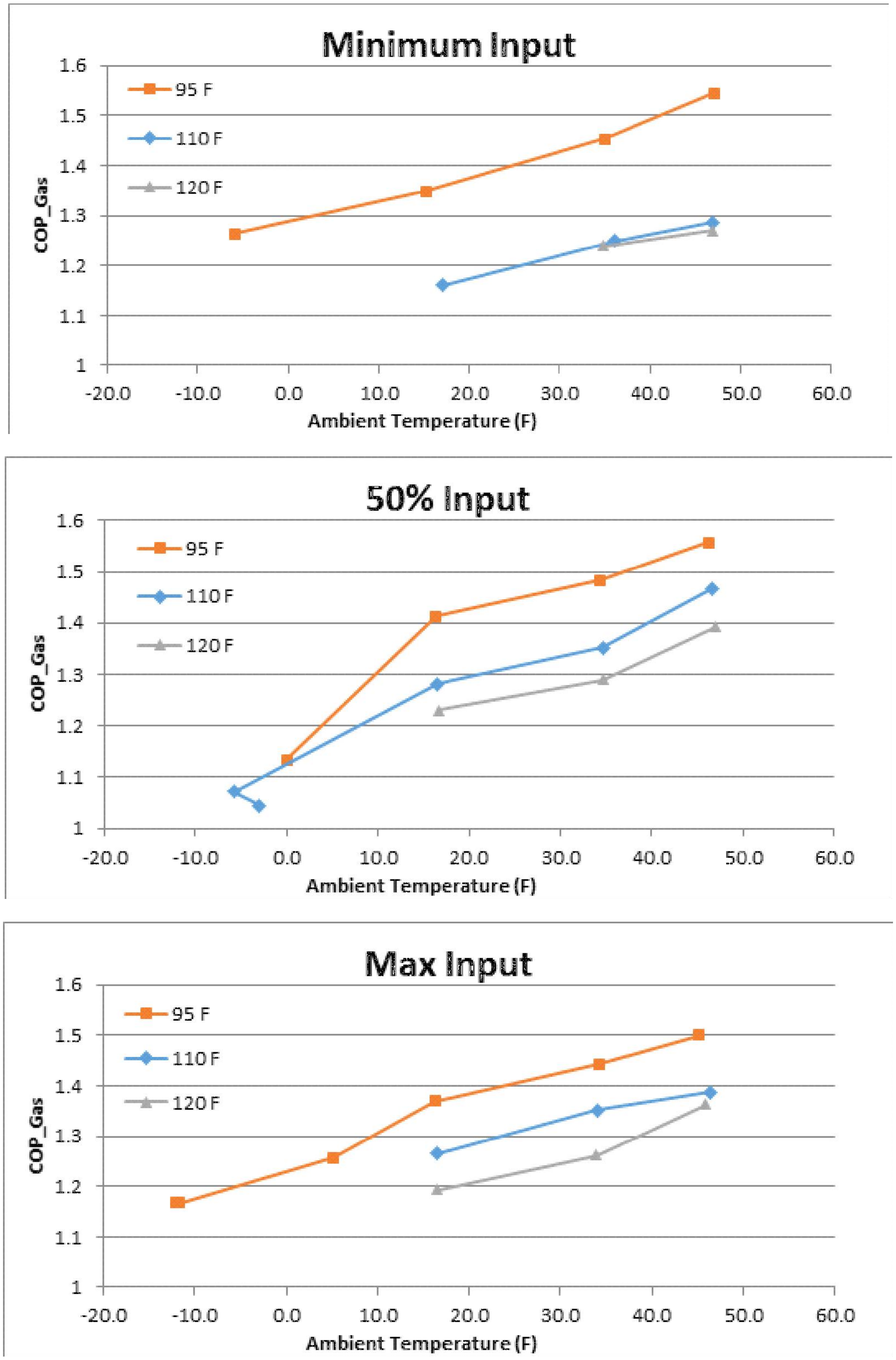

Figure 44: COP_gas versus Ambient Temperature

Table 5: Comparison of GAHP Performance to Goals

Ambient Temperature (°F)	COP_gas	Capacity (Btu/hr)	Hydronic ΔT (°F)
47	1.50	79,584	22.5
35	1.44	79,703	19.7
17	1.37	71,919	17.9
-13	1.17	55,746	14.7

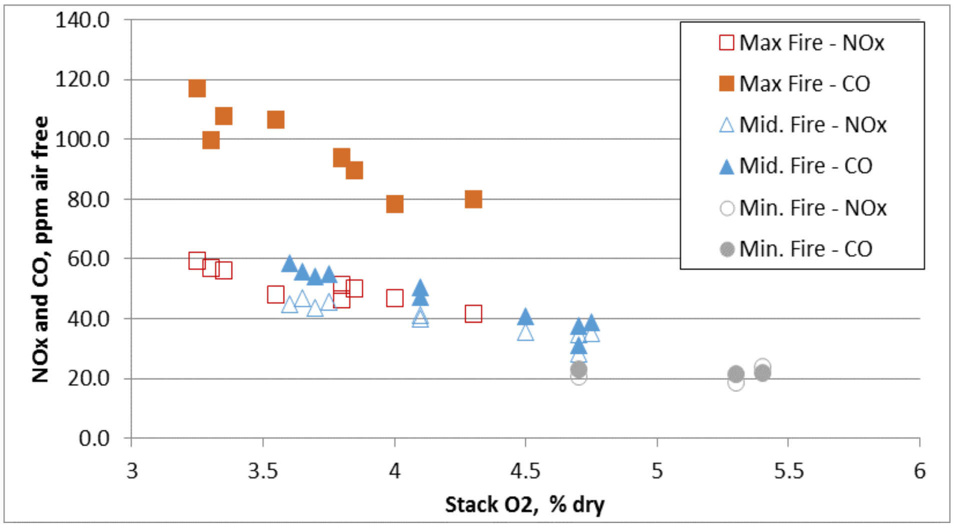

Figure 45: GAHP Emissions for Selected Test Points

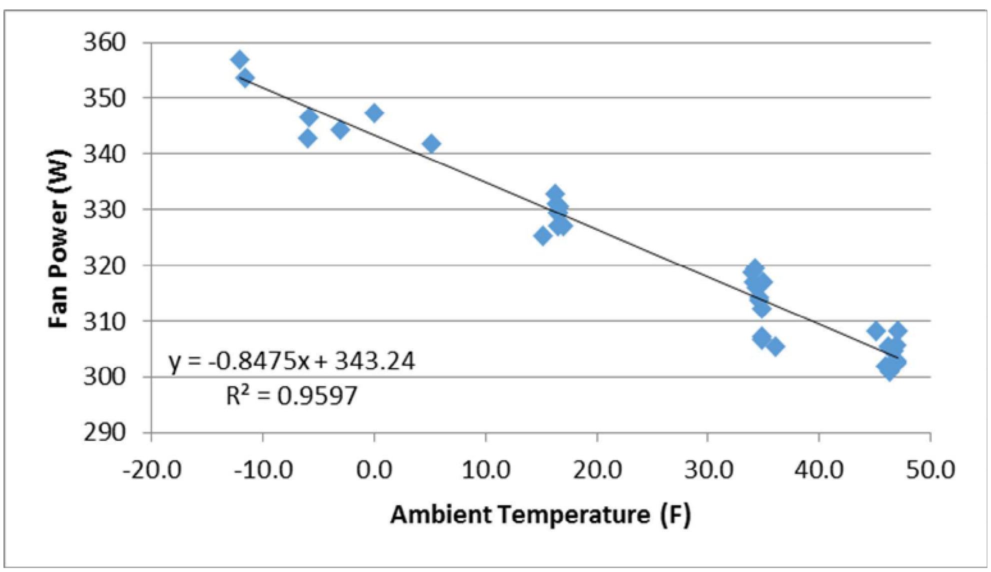

Figure 46: Evaporator Fan Power versus Ambient Temperature

12.0 Task 11: Building Energy Simulation

Description of Modeled Residential Homes

The heating load used to test the performance of the gas-fired absorption heat pump (GAHP) is derived from EnergyPlus model. Three prototypes [Ritschard et al. 1992] were simulated based on the year built and the main features of the modeled building from the Building American Benchmark 2010 (BA10) [Wilson et al. 2014]. Three locations, namely Albany NY, Minneapolis MN and Chicago IL, are modeled to obtain the space heating load for the three building prototypes. The annual average of the space heating loads are listed in [Ritschard et al. 1992] to show the difference between the modelled prototypes and BA10 building. The BA10 buildings are tight houses per standard IECC2009 and thus its heating load is approximately 45%, 56% and 73% of the prototypes A, B and C, respectively (Table 6).

Two installation types are selected as the baseline and they are boiler installation and furnace installations. A boiler with 100% AFUE is used in the boiler installation to generate the building heat demand for the GAHP system. When used for space heating alone, the GAHP with the heating capacity of 80,000 Btu/hr can be more suitable for retrofits of residential homes built before1980s (i.e. prototypes A and B).

Hybrid Module Simulating Gas Absorption Heat Pump Operation

A hybrid module was developed to simulate the operation of GAHP to meet the heat demand of a residential build derived from EnergyPlus. A hydronic return temperature is set by the user. The GAHP would meet the heat load first at the set point of the hydronic temperature by varying input percentage (i.e. modulation). If the input is below 25%, the hydronic temperature would increase until it reaches the temperature goal (i.e. 125°F). That is, if the load is too low and the input firing rate is below 25%, GAHP shuts down. If the input is at 100% but still the heat supply is smaller than heat demand, the hydronic return temperature will decrease. This process is implemented through electronic control system of the GAHP prototype and modeled in the hybrid module.

Table 6: Selected Locations and Heating Load

Location (BA climate zone)	Annual Average Heating Load by Building Type (Btu/hour)			
	BA10	A	B	C
Albany (5A)	5,891	13,454	10,912	7,998
Minneapolis (6A)	6,940	15,900	12,235	9,109
Chicago(5A)	5,590	12,087	9,777	8,245

Simulation Results and Discussion

Installation Types

The annual site energy savings for GAHP installed to replace boiler for hydronic heating and installed together with a hydronic furnace are studied and the results for three locations are shown in Figure 47. The annual savings comparison is against the energy used by a boiler of 100% site efficiency (i.e. electric boiler without accounting for the parasitic power consumed by the boiler). The results present the case with only natural gas consumed by GAHP (blue bars) and the case with both natural gas and electricity inputs (evaporator fan, solution pump, etc.) (red bars). Little difference is found between boiler-type installation and furnace- type installation. Such slight difference is caused by the heating load on GAHP in the air duct situation and hydronic loop setup. In both installation types, 22% to 37% energy saving is observed in building prototype A, 17% to 27% in building prototype B and 14% to 21% in building prototype C in the three locations. Given the similarity of the two installation types, boiler installation is used as the example in this report to demonstrate the performance.

It should be noted that the heat pump characteristics used in this analysis are from evaluation of the Alpha 1 unit. The reduction in parasitic power achieved by the Alpha 2 unit was not considered and would further improve the GAHP on-site energy savings. Improvement to system performance (expected had the absorber in Alpha 2 not been damaged) would also increase the energy savings offered by the GAHP.

Hydronic Return Temperature Setting

The effect of customer setting on hydronic return temperature of the GAHP prototype is illustrated in Figure 48 and the results show that the annual site energy saving increases with the decrease in hydronic return temperature set point. The GAHP prototype is designed to operate with the hydronic return flow first exchanging energy with combustion flue gas. The lower the hydronic return temperature, the more energy delivered from flue gas to the hydronic flow and the more energy from combustion is used for heating. Therefore, the GAHP energy efficiency is high as the return hydronic temperature decreases.

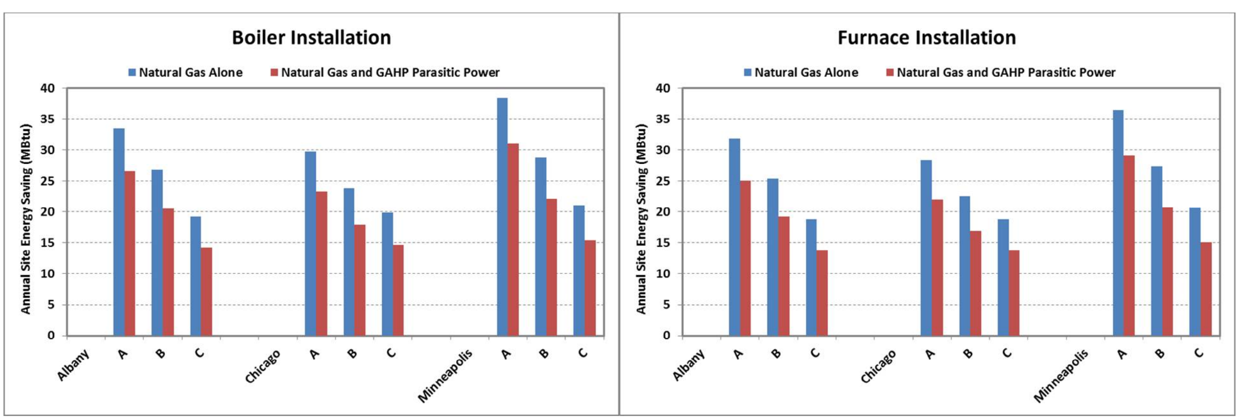

Figure 47: Annual Site Energy Saving Of GAHP for Two Installation Types (Baseline Is 100% Efficiency Boilers)

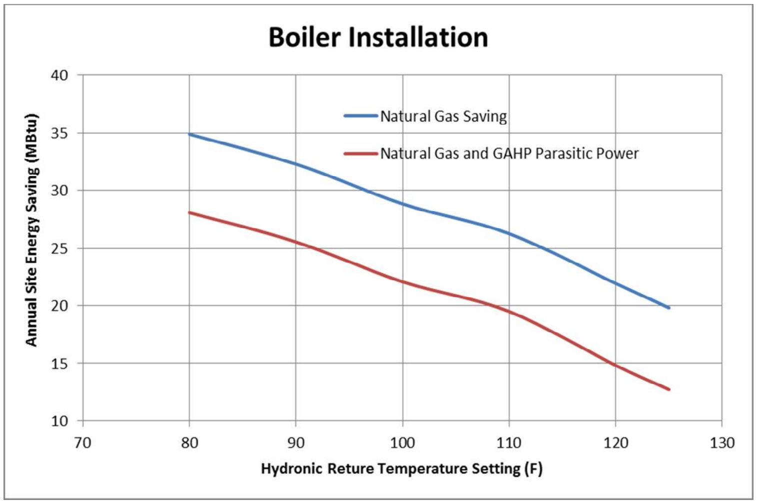

Figure 48: Effect of Hydronic Return Temperature Setting On Annual Energy Saving

Annual Performance for Building Prototype B

The GAHP performance including natural gas consumption, heat supply, gas COP and input percentage from January to December was investigated for building prototype B in Minneapolis. This building prototype was selected because the current GAHP prototype is designed for heat load of 80,000btu/h, a typical load of building prototype B. The GAHP system would be scaled for the designed heating load suitable to other two building prototypes. The simulation results for the other two cities have similar trends to those in Minneapolis. Overall, the GAHP prototype has an average COP of 1.4. The highest COP is approximately 1.5 and the lowest is approximately 1.2, highly depending on the ambient temperature.

The ambient temperature has significant impact on the annual operation. The outdoor dry bulb temperature of Minneapolis ranges from -20 to 98°F annually. There are two seasonal lows, one is in early winter and the other in late winter, December and February respectively. As demonstrated in the experimental data, gas COP decreases with the ambient temperature decreases. Thus, gas COPs corresponding to the two lowest outdoor temperatures are lower. On the days of these two lowest outdoor temperatures, the input percentage to GAHP reaches 100%. When the outdoor temperature is high in the heating season, the building load is reduced and GAHP would adjust its operation based on building load. For the period in the spring and fall when it is warm during the shoulder season (e.g. early May and October when it reaches around 80°F) the GAHP shuts down because of extremely low heating load and thus no heat is supplied. This is sometimes referred to for boilers as a “warm weather shutdown” or “WWSD”. Similar results were found for Albany and Chicago.

The annual energy saving of the GAHP prototype used in residential buildings were conducted and significant site energy savings are observed when used in the building type and the locations that this prototype is designed for. The average annual gas COP of approximately 1.4 was observed, consistent with the ANSI Z21.40.4 test results. When the ambient temperature increases, the heating load from the building is reduced and the GAHP will adjust its heat supply accordingly. As the heat load reduced to the level at which the input percentage is lower than the designed value, GAHP unit will have a “warm weather shutdown”.

13.0 Summary and Technology Status

A thermodynamic cycle model of a potentially low cost single-effect ammonia-water gas-fired absorption heat pump was modeled and optimized for residential and light commercial space heating. Breadboard testing was completed and allowed for design optimization of several key components. Two packaged prototype were designed, fabricated and tested (Alpha 1 and Alpha 2). Both prototypes were tested by SMTI and third party testing was performed on Alpha 1 by GTI. Energy use savings were then estimated based on the experimental data collected on the prototype units.

Measured prototype heat pump performance at the 47/100°F design condition is near the maximum for a single effect cycle. GTI testing and analysis of the Alpha 1 prototype predicted an AFUE of 136% for the climate region IV (outdoor design temperature of 5°F and 5,643 bin hours).

The prototype systems were able to achieve 4:1 modulation (target of 3:1). The parasitic electrical load was several hundred watts below the maximum target value of 750 watts. All sealed system components were fabricated with materials and methods that would allow for mass production and significantly reduced cost when compared to absorption heat pumps currently commercially available. Based on the projected cost of a production gas absorption heat pump based on the design developed under this program, and typical distribution channel mark-ups, the projected retail price will be 40-50% of an equivalent sized GAHP currently manufactured by Robur (Italy). This price level results in economic paybacks of 3-5 years compared to condensing furnaces.

SMTI is currently negotiating a commercialization agreement, initiating a 24-30 month product development phase to bring this technology to market by 2018.

14.0 REFERENCES

AHRI equipment shipment statistics, data accessed in 2015. Link: http://www.ahrinet.org/site/498/Resources/Statistics/Monthly-Shipments

Amrane, K., Sachs, H., and Nadel, S., "The Regional Standards Agreement for Residential Furnaces, Air Conditioners, and Heat Pumps: Progress, Results, and Implications", Proceedings of the ACEEE Summer Study on Energy Efficiency in Buildings, 2010.

ANSI Z21.40.4-1996 "Performance Testing and Rating of Gas-fired Air Conditioning and Heat Pump Appliances", American National Standard/Canadian Gas Association Standard, 1996 (Reaffirmed 2002).

Bibrzycki, J. and Poinsot, T. "Reduced Chemical Kinetic Mechanism for Methane Combustion in O2/N2 and O2/CO2 Atmosphere" Working note ECCOMET WN/CFD/10/17, CERFACS; 2010.

Caneta Research Inc., "Heat Pump Characterization Study", report prepared for Energy Solutions Centre and the Yukon Department of Energy, Mines, and Resources, 2010.

Cengel, Y.A. and A. J. Ghajar, "Heat and Mass Transfer: Fundamentals & Applications", 4th Edition. McGraw-Hill Companies, Inc, 2010.

Delta Energy & Environment & David Strong Consulting, "RHI Evidence Report: Gas Driven Heat Pumps – Assessment of the Market, Renewable Heat Potential, Cost, Performance and Characteristics of Non-Domestic Gas Driven Heat Pumps". Prepared for the UK DECC, 2014.

Department of Energy, Energy Information Administration. Residential Energy Consumption Survey, 2009 ed. http://www.eia.doe.gov/emeu/recs/contents.html

Department of Energy, Technical Support Document: Energy Efficiency Program For Consumer Products and Commercial and Industrial Equipment: Residential Furnaces, EERE-2014-BT-STD-0031-0027, February 10, 2015.

Friese, D. "CFD-Investigation of Absorption Heat Pump Heat Exchanger Designs and Performance", Bachelor Thesis, Department of Environmental Engineering, Technische Universitat Bergakademie Freiberg, 2015.

Garrabrant, M. "Development and Validation of a Gas-Fired Residential Heat Pump Water Heater - Final Report". 2013, prepared for the U.S. Department of Energy, Contract DE-EE0006116.

Huang, Ritschard, Bull , LBL-19128, "Methodology and Assumptions for Evaluating Heating and Cooling Energy Requirements in New Single-Family Residential Buildings", 1987.

Huang, J., Hanford, J., and Yang, F. "Residential Heating and Cooling Loads Component Analysis" Lawrence Berkeley National Laboratory LBNL-44636, 1999.

Kim, H., Baltazar, J.C., Haberl, J. "Methodology for Calculating Cooling and Heating Energy-Input-Ratio (EIR) from the Rated Seasonal Performance Efficiency (SEER or HSPF)", Texas A&M Energy Systems Laboratory, Report: ESL-TR-13-04-01, 2013.

Leslie, N., "Technical Analysis of DOE Notice of Proposed Rulemaking on Residential Furnace Minimum Efficiencies", Prepared by GTI for AGA and APGA, 2015. Link: https://www.aga.org/sites/default/files/21693_furnace_nopr_analysis_final_report_2015-07-15_00000002.pdf

Lima, Ricardo J. Da Silva and John R. Thome, "Two-Phase Frictional Pressure Drops In U-Bends And Contiguous Straight Tubes For Different Refrigerants, Orientations, Tube, And Bend Diameters: Part 1. Experimental Results" (RP-1444), HVAC&R Research, 18(6):1047-1071, 2012.

Lima, Ricardo J. Da Silva and John R. Thome, “Two-Phase Frictional Pressure Drops In U-Bends And Contiguous Straight Tubes For Different Refrigerants, Orientations, Tube, And Bend Diameters: Part 2. New Models” (RP-1444), HVAC&R Research, 18(6):1072-1097, 2012.

Ritschard, Handord, Sezgen, GRI-91/0236, LBL-30377, “Single-family heating and cooling requirements: assumptions, methods, and summary results”, 1992.

Wang CC, WL Fu, and CT Chang, “Heat Transfer and Friction Characteristics of Typical Wavy Fin-and-Tube Heat Exchangers”, Experimental Thermal and Fluid Science 14: 174-186, 1997.

Wilson, Metzger, Horowitz, NREL/TP-5500-60988, “2014 Building America House Simulation Protocols”, 2014.

Wojtan, L., Ursenbacher, T. and J.R. Thome, “Investigation Of Flow Boiling In Horizontal Tubes: Part I – A New Adiabatic Two-Phase Flow Pattern Map”. International Journal of Heat and Mass Transfer, 48: 2955-2969, 2005.

Wojtan, L., Ursenbacher, T. and J.R. Thome, “Investigation Of Flow Boiling In Horizontal Tubes: Part II – Development Of A New Heat Transfer Model For Stratified-Wavy, Dryout And Mist Flow Regimes”. International Journal of Heat and Mass Transfer, 48: 2970-2985, 2005.

Zurcher, O., Thome, J.R. and Favrat D.. “Evaporation Of Ammonia In A Smooth Horizontal Tube: Heat Transfer Measurements And Predictions”. Journal of Heat Transfer, 121: 89-101, 1999.

Zurcher, O., Favrat D. and J.R. Thome, “Evaporation Of Refrigerants In A Horizontal Tube: An Improved Flow Pattern Dependent Heat Transfer Model Compared To Ammonia Data”. International Journal of Heat and Mass Transfer, 45: 303-317, 2002.

15.0 List of Acronyms

AHRI	Air-Conditioning, Heating, and Refrigeration Institute
AOS	A.O. Smith
ASHRAE	American Society of Heating Refrigeration and Air-Conditioning Engineers
CEC	California Energy Commission
CFD	Computational Fluid Dynamics
CO	Carbon Monoxide
CO_2	Carbon Dioxide
COND	Condenser
COP	Coefficient of Performance
DES	Desorber
DOE	U.S. Department of Energy
EEV	Electronic Expansion Valve
EVAP	Evaporator
FEA	Finite Element Analysis
GAX	Generator Absorber Heat Exchanger (cycle)
GEN	Generator
GPM	Gallons Per Minute
GTI	Gas Technology Institute
HCA	Hydronically Cooled Absorber
HVAC	Heating, Ventilation and Air-Conditioning
ID	Inside Diameter
LBNL	Lawrence Berkeley National Laboratory
$LiBr\text{-}H_2O$	Lithium Bromide – Water (cycle)
LMTD	Log-Mean Temperature Difference
NAECA	National Appliance Energy Conservation Act
$NH_3\text{-}H_2O$	Ammonia – Water (cycle)
NIST	National Institute of Standards and Technology
NOx	Oxides of Nitrogen (NO2 + NO)
OD	Outside Diameter
PLC	Programmable Logic Controller
RFI	Request for Information
RHX	Refrigerant Heat Exchanger
SE	Single Effect (cycle)
SHD	Solution Heated Desorber
SHX	Solution Heat Exchanger
SMTI	Stone Mountain Technologies, Inc.
TC	Thermocouple
TE	Thermal Efficiency
UA	Overall Heat Transfer Coefficient x Heat Transfer Area
UA	Standby Heat Loss Coefficient (EF Test)
WC	(of) Water Column